Exploring the heterogeneous uptake of gas-phase PFCAs to the condensed phase

A thesis submitted to the Faculty of Graduate Studies in partial fulfillment of the requirements for the degree of

Master of Science

Graduate Program in Chemistry

York University

Toronto, Ontario August 2023

Abstract:

Perfluoroalkyl carboxylic acids (PFCAs) are a class of per- and polyfluoroalkyl substances (PFAS) which are completely fluorinated, accompanied by a carboxylic head functional group. These compounds are used in a variety of industrial and consumer products due to their beneficial chemical properties which include chemical inertness and thermal stability. These properties however lead to the slow and negligible degradation of these compounds in the atmosphere once they are released or formed through reactions of precursor molecules. With varying toxic effects on animals, plants, and humans, it has become imperative to understand the fate of these compounds in the atmosphere. The most important aspect in helping define a chemical's environmental fate is its physicochemical properties and partition tendencies. Partitioning of a gas phase chemical from air to water begins with the heterogeneous uptake of the gas-phase molecule onto the liquid's surface. Heterogeneous reactions are important in identifying sinks and the fate of atmospheric gas-phase chemicals. Uptake coefficients can be used to describe a chemicals heterogeneous uptake onto a liquid surface and are defined as the number of collisions that lead to uptake of a molecule. Currently there exists no experimental gas-phase uptake data for gas-phase PFCAs onto liquid surfaces which limits our understanding on their fate, movement, and sinks in the atmosphere. This work will aim to fill in gaps of knowledge for the heterogeneous uptake of a short chain PFCA, TFA, onto three liquid surfaces which include deionized water, saline water, and octanol. This work will also aim to calculate sampling efficiency for another short chain PFCA, PFPrA onto annular denuders coated with Na_2CO_3.

Acknowledgements

Firstly, I would like to thank my supervisor Cora Young for providing me with this opportunity and for mentoring me along this extended journey of mine. I also thank you for guiding and helping me gain confidence within the lab and within my project.

I thank my committee members, Cora Young, Trevor Vandenboer, and Robert McLaren for providing me with valuable feedback during my studies and research evaluations.

I want to give a special thanks to Teles Furlani and Leigh Crilley on being stand-out lab mates and helping me navigate the many issues experienced during the set-up of my experiments.

I also thank Eric Vanhauwaert for leading the analysis of bubbler samples for denuder sample efficiency experiments on the IC-CD.

Table of contents

Abstract……. ii

Acknowledgements……..... iii

Table of contents…….. iv

List of tables and figures……. vi

List of symbols and abbreviations……. vii

Chapter 1: Introduction……... 1

1.1 Introduction to PFAS and PFCAs…… 1

1.2 Occurrence in the atmosphere and other environmental compartments……..……. 4

1.3 Methods of atmospheric sampling…… 6

1.4 Factors and processes affecting fate of gas-phase PFCAs in the atmosphere…….. 8

1.5 Our current knowledge on the chemical properties of PFCAs……... 10

1.6 Instrumentation……... 11

1.7 Objectives of proposed research……. 14

References……. 15

Chapter Two: Calculation of gas-phase uptake coefficients for TFA on various liquid surfaces using chemical ionization – mass spectrometry…… 19

2.1 Introduction……. 20

2.2 Materials and Methods…… 21

2.2.1 Calculating uptake coefficients…… 23

2.3 Results and Discussion……... 25

2.3.1 Atmospheric implications…… 31

References……. 33

Chapter Three: Sampling efficiency of gas-phase PFPrA using Na_2CO_3 coated annular denuders……...… 35

3.1 Introduction……. 36

3.2 Materials and Methods…… 37

3.2.1 Preliminary denuder efficiency experiment (TFA/CI-MS)……..... 37

3.2.2 Denuder sample efficiency experiments and calculations (PFPrA/IC-CD)…… 39

3.3 Results and Discussion……... 41

3.4 Atmospheric implications……... 44

References……. 45

Chapter Four: Conclusions and future work……... 47

References……. 50

List of tables and figures

Figure 1-1. TFA, PFPrA, and PFBA, examples of short-chain PFCAs

Figure 1-2. Processes which determine the net uptake of a gas onto a liquid surface

Figure 1-3. Schematic of chemical ionization mass spectrometer

Figure 1-4. Schematic of ion chromatography – conductivity detection

Figure 2-1. Schematic of flow tube setup for reactive uptake experiments involving TFA

Figure 2-2. Visual diagram of glass injector being inserted and pulled out from the flow tube

Figure 2-3. Reactive uptake of TFA onto various surfaces (injector pulled out). The green line represents the blank, blue represents deionized water, orange/yellow represents saline water, and red represents octanol. C_t/C_0 represents the acetate normalized signal of TFA normalized to the beginning of the run. Shading represents the standard deviation.

Figure 2-4. Reactive uptake of TFA onto various surfaces (injector pushed in). The green line represents the blank, blue represents deionized water, orange/yellow represents saline water, and red represents octanol. C_t/C_0 represents the acetate normalized signal of TFA normalized to the beginning of the run. Shading represents the standard deviation.

Figure 3-1. Schematic of preliminary denuder efficiency experiments using TFA/CI-MS. Lines 1 and 2 were not interchangeable (only one line was running at a time)

Figure 3-2. Schematic of official denuder efficiency experiments using PFPrA/IC-CD. Lines 1 and 2 were not interchangeable (only one line was running at a time)

Figure 3-3. Preliminary denuder efficiency experiment involving TFA and CI-MS

Table 2-1. Range of calculated uptake coefficients for TFA on the surface of deionized water, saline water, and octanol.

Table 2-2. Comparison of uptake coefficients for TFA, HCl, and HNO3 on the surface of water

Table 3-1. Calculated lower limits of denuder sampling efficiency for each set of PFPra bubble samples analyzed using IC-CD

List of symbols and abbreviations

±	plus-minus
%	percent
>	greater than
<	less than
◦C	degree Celsius
“	inch
a	mass accommodation coefficient
γ	measured uptake coefficient
C2-C15	carbon chain length (2-15)
CI-MS	chemical ionization – mass spectrometer
cm	centimeter
FTOH	fluorotelomer alcohol
GFF	granite fiber filters
H^+	hydronium ion
HCl	hydrochloric acid
HCFC	hydrochlorofluorocarbon
HFC	hydrofluorocarbon
HNO_3	nitric acid
IC-CD	ion chromatography – conductivity detection
K_{AW}	air-water partition coefficient (Henry’s law constant)
K_{OW}	octanol-water partition coefficient
K_{OA}	octanol-air partition coefficient
K	kelvin
kg	kilogram

L	litre
LOD	limit of detection
MFC	mass flow controller
mL	millilitre
m	meter
mm	millimeter
m^3	cubic meter
m/z	mass to charge ratio
N/A	not applicable
NaOH	sodium hydroxide
Na_2CO_3	sodium carbonate
OH^-	hydroxide
PFAS	perfluoroalkyl substance
PFCA	perfluorocarboxylic acid
PFPrA	perfluoropropionic acid
PFBA	perfluorobutanoic acid
PFPeA	perfluoropentanoic acid
PFHxA	perfluorohexanoic acid
PFHeA	perfluoroheptanoic acid
PFOA	perfluoro-octanoic acid
PFNA	perfluorononanoic acid
PFDA	perfluorodecanoic acid
pg	picogram
pH	scale of acidity, $-\log(H^+)$
pKa	acid dissociation constant

PFA	perfluoroalkoxy alkane
ppb	part per billion (ug/L)
ppt	part per trillion (ng/L)
PUF	polyurethane foam
PTFE	polytetrafluoroethylene
QFF	quartz fiber filter
sccm	standard cubic centimeter per minute
TFA	trifuluoroacetic acid
µg	microgram
XAD	styrene divinyl-benzene copolymer

1.1 Introduction to PFAS and PFCAs

Per- and polyfluoroalkyl substances (PFAS) are a class of compounds in which carbon-hydrogen bonds are partially or completely replaced with fluorine-carbon bonds. In general, these compounds can be described as having at least one fully fluorinated methyl or methylene carbon atom without hydrogen, chlorine, bromine, or iodine attached to it (Wang et al. 2021). Perfluoroalkyl substances are used in a wide variety of applications such as non-stick cookware, food packaging, fabrics and carpets, cosmetics, and firefighting foams due to the beneficial properties they can lend to consumer and industrial products. Some of these beneficial chemical properties include chemical inertness, hydrophobicity, and low surface tension (Gluge et al. 2021). Consequently, upon being released into the environment, these compounds are subject to slow or negligible environmental degradation and are thus considered an emerging class of pollutants capable of bioaccumulation in wildlife, persistent global buildup, long range transport, toxic effects in animals, and increasing human exposure. Some toxic effects of PFAS in humans and other animals include various forms of cancer, and liver damage. These chemicals can also have effects on unborn fetuses and lead to increased miscarriage risks. The main factors affecting toxicity, transport/fate, and bio-accumulative potential in PFAS include the degree of fluorination, carbon chain length, and functional groups present within the molecule (Lau et al. 2004; Lau et al. 2006)

One subclass of PFAS that has attracted attention recently due to its toxicity, bioaccumulation in wildlife and plants, and ubiquitous presence within the atmosphere, water bodies, and human beings includes perfluoroalkyl carboxylic acids (PFCAs). This subclass of PFAS can be described as being fully fluorinated whereby carbon-hydrogen bonds are completely replaced with carbon-fluorine bonds, accompanied by a carboxylic acid functional head group. Perfluoroalkyl carboxylic acids can be further categorized by chain length with PFCAs that have a carbon chain length longer than seven being considered long chain. Those with seven or fewer carbons are considered short chain while PFCAs with four or fewer carbons are considered ultra-short chain. Like other PFAS, PFCAs were manufactured for use due to their unique chemical properties which included water/oil repellency and thermal stability (Wang et al. 2013). Examples of three ultra-short chain PFCAs which include trifluoroacetic acid

(TFA), perfluoropropionic acid (PFPrA), and perfluorobutanoic acid (PFBA) are given below in Figure 1-1.

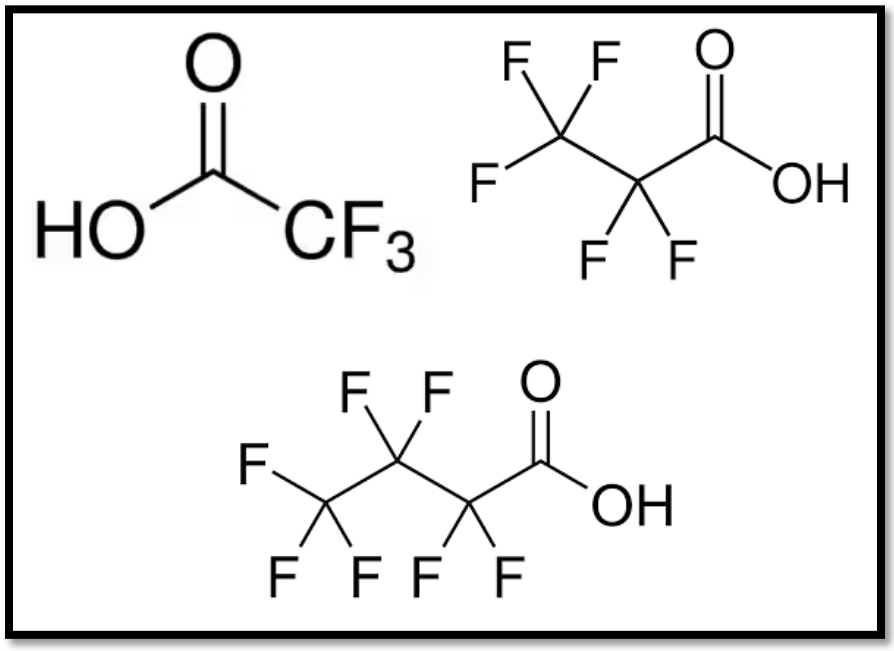

Figure 1-1. Chemical structures of TFA, PFPrA, and PFBA, examples of ultra-short chain PFCAs

Historically, PFCAs (specifically long chain PFCAs which had carbon chain lengths ranging from 8-11 carbons) have been used in a number of consumer products and industrial processes. An important process utilizing PFCAs involved their use as processing aids in the (emulsion) polymerization of fluoropolymers such as polytetrafluoroethylene (PTFE), perfluorinated ethylene-propylene copolymer (FEP), and perfluoroalkoxy polymer (PFA) (Prevedouros et al. 2005). Perfluoroalkyl carboxylic acids are also used in surface treatment products to impart water and oil resistance to leather, textiles, carpets, and food packaging, as well as surfactants in aqueous firefighting foams (Prevedouros et al. 2005). Over time, the production and use of long chain PFCAs, such as perfluorooctanoic acid (PFOA) have been decreased due to evidence of their increased potential for bioaccumulation and environmental

persistence compared to shorter chain PFCAs. This has led to the increased use of shorter chain PFCAs which include PFBA, as well as other fluorinated alternatives (Prevedouros et al. 2005).

These industrial processes and consumer products act as direct emission sources of PFCAs into the atmosphere, however these direct emissions only account for a relatively small portion of total PFCAs in the atmosphere, specifically in remote regions (Young, et al 2010). This is because PFCAs are strong acids and are therefore expected to exist in their ionic form under most environmental conditions and pHs (Thackray et al. 2020). Strong acids have high solubility in water and negligible vapor pressures in their ionized form, meaning they will most likely be scavenged from the atmosphere by cloud droplets and deposited to the Earth's surface, ionizing in solution and preventing long range transport into remote regions. A small portion of PFCAs emitted from direct sources are likely to partition to the particle phase (aerosols) allowing for longer range transport compared to gas-phase PFCAs (Tao et al. 2022). Atmospheric lifetimes of water soluble gases against wet deposition are considered to be on the orders of days. One previous study, using the 3-D global chemistry transport model, STOCHEM-CRI, estimated the atmospheric lifetime of gas-phase acetic acid with respect to wet deposition to be 1.6-1.8 days (Anwar et al 2018). Atmospheric lifetimes of aerosol particles can vary from days to months, dependant primarily on the size of the particles and the height at which they are injected into the atmosphere. Fine aerosol particles generally have longer atmospheric lifetimes as compared to coarse aerosol particles. Aerosol particles injected within the boundary layer also generally have shorter atmospheric lifetimes compared to those injected aloft into the upper troposphere. In general, the importance between wet and dry deposition for removal of gas-phase PFCAs in the atmosphere is likely most pronounced above the boundary layer (upper troposphere and lower stratosphere). That is, partitioning to aerosols will be more important as compared to heterogeneous processes such as uptake into rain/cloud droplets. This is because at higher altitudes, lower temperatures and decreased water vapor concentrations favor the formation of aerosols, leading to the increased partitioning of PFCAs onto aerosol surfaces. Examples of this can be given using observations made for other strong atmospheric acids, such as nitric acid (HNO_3). A recent study using both in situ measurements and model predictions demonstrated that nitrate aerosol mass fractional contribution to aerosols is significantly higher in the upper troposphere (30-40%) compared to near the surface (6%) where removal is dominated by wet deposition (Yu et al 2022).

Recent measurements of PFCAs from an ice core in the remote Arctic demonstrated a correlation between several PFCAs and non-sea salt calcium and magnesium which are two components of primary (mineral dust) aerosol and suggest these kinds of aerosols could have contributed to their presence in the remote regions (Pickard et al. 2018). Mineral dust aerosol is generated due to the physical weathering of minerals (such as limestone) and blowing of sand/dry soil via wind. The largest portions of mineral dust in the atmosphere originate from dry and dessert regions. Another type of primary atmospheric aerosol includes sea spray aerosol which is generated from the bursting of air bubbles over the ocean's surface and is mostly composed of sea salt but also consists of dissolved organic carbon. It has been suggested that PFCAs can be transported long distances via oceanic transport with recent publications finding that some PFCAs can be re-emitted from surface ocean water back into the atmosphere through the generation of sea spray aerosol (Sha et al. 2022; Johanson et al. 2019). It was determined however that oceanic transport did not contribute to concentrations of PFCAs in the remote arctic through measurements of PFCAs from the Devon Ice Cap. Sodium (Na^+) quantified in ice cores was assumed to come from sea salt while most of the other ions were attributed to the non-sea salt component. It was also noted that no correlations were observed between the Na^+ flux and any PFCAs, suggesting limited oceanic sources depositing on the Devon Ice Cap (Pickard et al. 2018). Other types of atmospheric aerosols which may have an impact on the transport of of gas-phase PFCAs in the atmosphere include smoke and industrial aerosols. Smoke mainly originates from wildfires and biomass burning and is composed mostly of organic and black carbon. Industrial aerosols originate from industrial combustion processes (such as coal burning) and consist of sulfates, nitrates, and organic and black carbon. Depending on the composition (mineral dusts, sea spray, smoke, industrial) and meteorological conditions, phase separation between water insoluble organic and aqueous phases can have an impact on the partitioning/movement of water soluble gas-phase molecules (You et al. 2012; Song et al. 2017).

Another scenario in which PFCAs can be transported to remote regions includes the transformation of precursor molecules. Atmospheric PFCA precursors such as fluorotelomer alcohols (FTOHs), hydrofluorocarbons (HFCs), and hydrochlorofluorocarbons (HCFCs) have much longer atmospheric lifetimes (on the order of weeks/months for FTOHs and years for HFCs and HCFCs) compared to PFCAs, allowing these chemicals to be transported long distances into remote regions. These chemicals can then undergo oxidation reactions with

photochemically important species such as the hydroxyl radical to produce significant portions of gas phase PFCAs in the atmosphere (Young et al. 2010; Thackray et al. 2020). Multiple HCFCs and HFCs (HCFC-123, and HCFC-124, and HFC-134a) have been reported to produce varying amounts of TFA through atmospheric oxidation reactions (Solomon et al. 2016). Atmospheric conversion rates of HCFC-123 and HCFC-124 into TFA have been calculated to be close to 100% while conversion of HFC-134a into TFA has been found to vary anywhere between 7-21%. Other fluorinated compounds have also been found to produce PFCAs through chemical transformations in the atmosphere with another study documenting a 100% conversion of 2,3,3,3-tetrafluoropropene (HFO-1234yf), a replacement for HFC-134a, into TFA (Solomon et al. 2016). In different atmospheric environments, these photochemical and precursor species vary over orders of magnitude, affecting the ability of the atmosphere to produce PFCAs (Young et al. 2010; Thackray et al. 2020; Solomon et al. 2016). In general, the long-range transport of PFCAs to remote regions such as the Arctic is attributed solely to the atmospheric transformation of these various precursor species (Pickard et al. 2018; Pickard et al. 2020).

1.2 Occurrence in the atmosphere and other environmental compartments

As of now, PFCAs with chain lengths ranging from two carbon atoms to more than fourteen carbon atoms have been detected and quantified in various environmental samples along with their chemical precursor species. Concentrations of these compounds in dry (gas and aerosol) and wet (rainwater) deposition samples have been found to vary greatly depending on location (i.e., urban or remote) and time of year. Several past studies have documented concentrations of various PFCAs in atmospheric air samples. One study recorded the spatial distribution of the sum of five PFCAs in urban and remote locations in Canada. It was found that the air concentrations of the sum of measured PFCAs were highest in Toronto, ON (0.44 pg/m^3) in 2009, followed by Lake Superior (0.075 pg/m^3) in 2009 and the remote Arctic sites (0.06 pg/m^3, 0.050 pg/m^3, and 0.014 pg/m^3 for Labrador Sea (2007), Hudson Bay (2007), and Beaufort Sea (2008), respectively) (Gewurtz et al. 2013). Concentrations of PFCAs were recorded in another remote Canadian Arctic site (Cornwallis Island). Among all PFCAs measured (C7-C15) the dominant PFCAs observed were determined to be PFOA (1.4 pg/m^3), followed by perfluorononanoic acid and perfluorodecanoic acid (0.4 pg/m^3). Concentrations of

PFOA were also quantified in particulate matter during this campaign with concentrations ranging from 0.1 – 3.84 μg/m^3 (Stock et al. 2007). Measurements of PFCAs have also been made outside of Canada within much more densely populated areas such as China. A study conducted in Beijing; China documented air concentrations of total PFCAs ranging from 53 – 800 pg/m^3 (Wu et al. 2019). Among all measured PFCAs, perfluoropentanoic acid was dominant (43–830 pg/m^3), followed by perfluoroheptanoic acid (2.7–31 pg/m^3) and PFBA (1.2–23 pg/m^3). It has been noted however that TFA and PFPrA were not measured in these studies. More recent studies which have included TFA and PFPrA in atmospheric measurements alongside other PFCAs have observed TFA as the most abundant gas-phase PFCAs in the atmosphere followed by PFPrA, with concentrations ranging from 15-426 pg/m^3 (Ye et al. 2023). It was also found that concentrations of these PFCAs were highest during the summer months and lowest during the winter (Wu et al. 2019). Temporal trends of PFCAs in the atmosphere have been established, with total deposition fluxes (ug/m^2 yr) of short and long chain (C2-C11) PFCAs increasing dramatically over the course of the past 30 years, beginning in 1990 with the enactment of the Montreal Protocol (Pickard et al. 2020; Garnett et al. 2022; Young et al. 2007). Rainwater samples have previously been collected and analyzed for PFCAs with increasing concentrations with decreasing chain length. In one study concentrations of TFA, PFPrA, and PFBA were found to be 1-2 orders of magnitude larger than longer chain PFCAs (>C5), with TFA having the largest concentrations out of all PFCAs analyzed (C2-C12) (Taniyasu et al. 2008).

Water (lakes/oceans/rivers) are another environmental compartment in which PFCAs have been quantified in. A recent investigation of PFCAs in the great lakes reported concentrations less than 10 ng/L, levels like the concentrations detected in those of remote Arctic lakes (Amituk/Char Lake). However, elevated concentrations of PFCAs were detected in two separate urban and rural locations which included Hamilton Harbor and Resolute Lake with concentrations that were approximately 3-4 times higher than those found in the Great lakes (Stock et al 2007). Concentrations of PFCAs measured in open waters of the Pacific and Atlantic Oceans (0.1−429 pg/L) were also found to be an order of magnitude smaller than those found in Amituk/Char Lake and of those found in the Great Lakes (So et al. 2004; Yamashita et al. 2005).

Plants, animals, and humans have also become important environmental compartments for which PFCAs can accumulate. Short chain PFCAs, specifically TFA, PFPrA, and PFBA has

been found to accumulate in plants, including crops for human consumption (Guckert et al. 2023). As such, it has been found that the highest concentrations of short chain PFCAs (especially TFA) are found in tissues of herbivorous and omnivorous animals such as deer and boar. Longer chain PFCAs (especially PFOA) have been found to dominate in carnivorous animals such as otters with total PFCA concentrations increasing dramatically as you move up the trophic food web (Guckert et al. 2023). Measurements of PFCAs in human serum have also been reported whereby TFA concentrations were found to be larger than all other PFCAs except for PFOA (Duan et al. 2020).

1.3 Methods of atmospheric sampling

Air samples of PFCAs can be collected using both passive and active sampling methods. Passive air samplers collecting trace atmospheric acids such as PFCAs have utilized polyurethane foam (PUF) disks, often with another sorbent added (Shoeib et al. 2008). Polyurethane foam disk passive air samplers have been effective in spatial air mapping studies of hydrophobic chemicals (such as PFCAs) without the need of electricity or expensive air sampling equipment (Shoeib et al. 2008). However, with the knowledge that PFCAs also exist in the particle phase, high/medium volume samplers have become the preferred method of sampling due to their ability to capture both gas and particle phase PFCAs separately. In past studies medium/high volume active samplers have utilized glass fiber filters (GFFs) and quartz fiber filters (QFFs) to sample PFCAs in the gas and particulate phase for their ability to strongly sorb atmospheric acids. Although advantageous, many disadvantages were also reported which included the presence of positive sampling artifacts (Ahrens et al. 2011; Ahrens et al. 2012).

The presence of positive sampling artifacts demonstrated that gas-phase PFCAs can adsorb to GFFs or QFFs and particulate matter already collected on the filter using conventional high volume sampling techniques. This resulted in an overestimation of the particle phase concentration (blow-on sampling artifact) (Ahrens et al. 2011; Ahrens et al. 2012). These conventional samplers are also susceptible to potential blow-off sampling artifacts whereby chemicals adsorbed on particulate matter can be volatilized from the particles after collection on GFF which results in a decreased particle phase concentration. It was also noted that both effects

can occur simultaneously. To avoid these sampling artifacts a new type of sampler, the annular diffusion denuder, was implemented to be used for PFAS alongside high/medium volume samplers. Annular diffusion denuders can be described as multichannel tubes made of glass and coated with a compound such as Na_2CO_3 or XAD-4 resin which aid in the adsorption of gaseous acids and volatile organic compounds respectively (Ahrens et al. 2011; Ahrens et al. 2012). The diffusion denuder sampler avoids these sampling artifacts by collecting the gas-phase first followed by the particle-phase, preventing the gas and aqueous phase adsorption of PFCAs to GFFs and QFFs.

Several previous studies have investigated the use of denuders for sampling gas-phase PFCAs in the atmosphere. One study, using XAD-4 coated annular denuders, sampled several short and long chain PFCAs (C4-C12, C14) in Toronto, ON. Fourteen pairs of annular denuder samples were collected alongside traditional high-volume samplers (PUF/XAD-2 cartridges) for 24 hr periods (Ahrens et al. 2011). Denuder samples were extracted using petroleum ether, followed by methanol, and analyzed using liquid chromatography interfaced with a triple quadrupole mass spectrometer in negative ion mode (LC-ESI-MS/MS). Concentrations of PFCAs sampled using annular denuders were, in general, found to decrease with increasing chain length and ranged from ~0.5 pg/m^3 – 15 pg/m^3. Out of all PFCAs, PFBA was found to have the largest denuder concentrations (~15 pg/m^3). Concentrations of PFCAs using traditional high volume sampling methods were found to be smaller than those quantified using annular denuders. Average recoveries were 81% and 66% for gas-phase compounds using the diffusion denuder and high-volume air samplers, respectively (Ahrens et al. 2011). For the particle-phase, average recoveries were 87% for either sampling technique. A key difference between both techniques is that the high-volume air sampler measurements resulted in higher particle-associated fractions (64-100%) of C8−C14 PFCAs compared to the diffusion denuder sampler (6-61%). This demonstrated issues associated with the use of traditional high volume sampling techniques for assessing gas-particle partitioning of certain PFCAs due to gas-phase sorption of the chemical onto the GFF (Ahrens et al. 2011). Another previous study, using Na_2CO_3 coated denuders, also sampled several short and long chain PFCAs (C2-C14) in Toronto, ON. Denuder samples were collected for a total of one month from September to October (Ye et al. 2023). Denuder samples were extracted using deionized water and analyzed using gas-chromatography interfaced with a mass spectrometer (GC-MS). Concentrations of PFCAs were once again found

to decrease with increasing chain length and ranged from 426 pg/m^3 – 0.15 pg/m^3. Out of all PFCAs, TFA was found to have the largest denuder concentrations (426 pg/m^3). Average recoveries for denuder samples ranged from 50% - 121% with the lowest recoveries observed in long chain PFCAs (>C10) (Ye et al. 2023).

While the use of denuders has improved the accuracy of atmospheric sampling of PFCAs, timescales for these measurements are slow (on the order of days to weeks). Therefore, understanding the processes which help determine the atmospheric fate of PFCAs requires faster measurements.

1.4 Factors and processes affecting fate of gas-phase PFCAs in the atmosphere

Movement/transfer of a chemical from one compartment to another can be described in terms of both heterogeneous and equilibrium processes. Many important atmospheric reactions involve heterogeneous interactions of gas-phase species with water droplets and aerosols. Recognition of the importance of such heterogeneous processes has attracted an increasing amount of interest in this field and how it can help understand atmospheric sinks and fate for gas-phase chemicals. Heterogeneous processes begin with the gas molecules colliding with the surface of water droplets and aerosols, followed by entering the condensed phase (Figure 1-2). An important parameter that determines the transfer rate of gases into atmospheric water droplets and aerosols is the mass accommodation coefficient (a) which is the probability that an atom or molecule striking a liquid surface enters the liquid phase. In most circumstances, other processes are also involved in and can influence gas uptake onto a liquid surface. Some of these processes include diffusion of the trace species through the gas phase to the surface, adsorption and desorption at the surface, solvation of the species and incorporation into the bulk phase, and reaction at the surface and in the bulk phase (Figure 1-2). In experiments subject to these processes, the measured flux into a liquid is expressed in terms of a measured uptake coefficient (γ) (Davidovits et al. 2006; Tang et al. 2014).

In situations where the uptake at the surface is high, the gas-phase concentration near the surface can decrease if diffusion in the gas phase is too slow to replenish the molecules. This in turn limits the gas uptake by the liquid. After the molecule enters the liquid, it diffuses away

from the surface into the bulk liquid. However, the capacity of the liquid to accommodate a gas molecule is also limited by the capacity of the liquid to solvate the gas molecules, and for these molecules to diffuse into the liquid. Therefore, a fraction is expected to evaporate back into gas phase due to solubility limitation (Davidovits et al. 2006; Tang et al. 2014). Both gas phase diffusion and solubility limitations can lead to an effective uptake coefficient which in turn is smaller than the true uptake coefficient. With time, the molecules in the liquid-phase equilibrate with the gas phase. At equilibrium, the rate of molecules desorbing from the surface is equal to the rate of molecules accommodating at the surface, yielding a net uptake of zero.

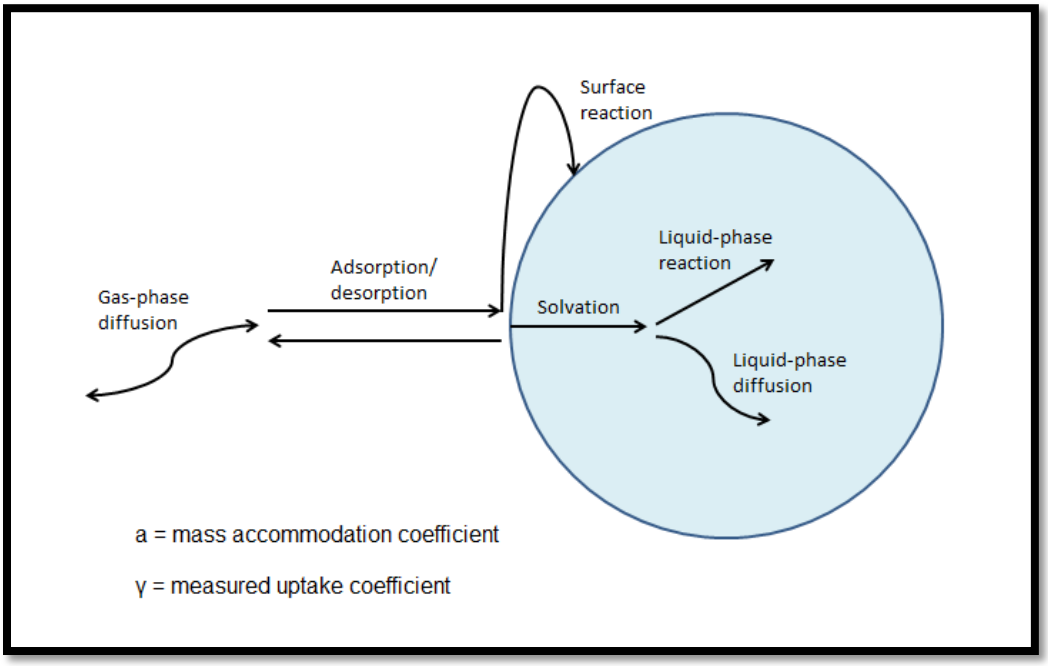

Figure 1-2. Processes which determine the net uptake of a gas onto a liquid surface

Once at equilibrium, the movement of a chemical between two compartments such as air and water can be described in terms of equilibrium partitioning. The partitioning tendencies for gas phase chemicals at equilibrium within the atmosphere are determined by three equilibrium partition coefficients between air-water (K_{AW}), octanol-water (K_{OW}), and octanol-air (K_{OA}) (Parnis et al. 2020). These partition coefficients can be defined as a dimensionless ratio of a chemical's equilibrium concentration in two different compartments (e.g. $K_{AW} = C_{air} / C_{water}$) and

are commonly used to estimate the environmental fate of chemicals. Octanol serves as a substitute for hydrophobic media such as organic matter in water/aerosol particles and tissues in biota. Factors affecting equilibrium partitioning of a chemical between two media include pH which is important for ionizable species, temperature, and salinity (Parnis et al. 2020).

1.5 Our current knowledge on the chemical properties of PFCAs

In general, only a handful of experimental data exists on the chemical properties/partition tendencies for PFCAs. Attempts have been made to measure various chemical properties of PFCAs; however, their surfactant-like nature has resulted in certain chemical properties being difficult to measure accurately. The high degree of fluorination in these molecules also makes it difficult to accurately estimate chemical properties using thermodynamic/solvation theory models, resulting in values differing by orders of magnitude. A particularly challenging property to experimentally determine is the octanol–air partition ratio, K_{OA} (Parnis et al. 2020). Chemical properties which have been experimentally determined in the past for a small number of PFCAs include pKa, vapor pressure, solubility, K_{OW}, and K_{AW} (or Henry's law constant) (Mackay et al. 2007; Kutsuna et al. 2008; Kaiser et al. 2005; Xiang et al. 2018; Moroi et al. 2001; Goss et al. 2008; US EPA. 2019). Dissociation constants (pKa) are independent of carbon chain length and have been found to vary only slightly among short and long chain PFCAs (Moroi et al. 2001; Goss et al. 2008; Wang et al. 2011). Vapor pressures for several short and long chain PFCAs have been found to decrease with increasing carbon chain length (Kaiser et al. 2005). Solubility in water also follows the same pattern as vapor pressure whereby solubility decreased with increasing carbon chain length (US EPA 2019). Air-water (K_{AW}) and octanol-water partition ratios (K_{OW}) for various length PFCAs have been previously reported as well whereby K_{OW} and K_{AW} increased with increasing chain length. This indicates that short chain PFCAs are more likely to persist in water while longer chain PFCAs are more likely to be found in the gas and particle phase (Mackay et al. 2007; Kutsuna et al. 2008; Xiang et al. 2018). In terms of heterogeneous processes, there exists little to no experimental data on the uptake of gas phase PFCAs onto liquid surfaces. This lack of experimental kinetic data limits our understanding on the speed at which these heterogeneous atmospheric processes involving gas-phase PFCAs

occur. This lack of kinetic data also limits our understanding on the movement of gas-phase PFCAs within the atmosphere and their possible sinks.

1.6 Instrumentation

1.6.2 Ion exchange chromatography – conductivity detection

Ion Chromatography (IC) is a separation method used for ionic and polar analytes based on their interactions with a mobile and stationary phase. There are two types of IC: anion and cation exchange. Anion exchange is used to separate ions which are negatively charged while cation exchange is used for those that are positively charged (Fritz et al. 2000). Anion exchange chromatography uses buffers containing salts for the mobile phase (NaOH in most cases) which are used to carry analytes through the chromatography column packed with a stationary phase. The stationary phase consists of positively charged exchange functional groups (quaternary ammonium in the case of anion exchange) that interact with the analytes. The higher the surface charge density on the analyte, the stronger the electrostatic attraction to the positively charged exchange functional groups on the stationary phase. For anion exchange, a salt gradient (increase in ionic strength) is used to elute negatively charged ions that have been bound to the stationary phase. As the ionic strength of the mobile phase increases the ions in the elution buffer compete for and replace the analytes at the charged sites on the stationary phase surface. At low ionic strength, weakly bound analytes (molecules having lower surface charge densities) start eluting from the column. As ionic strength is increased, strongly bound molecules with increasingly higher surface charge densities elute from the column (Fritz et al. 2000).

To begin, the eluent is degassed to maintain a constant pH and the analytical column is equilibrated with this degassed eluent to create a stable baseline. Samples are transferred by the auto sampler into the sample loop and injected onto the column for separation. A guard column is placed before the analytical column to extend the lifetime of the analytical column by filtering out any contaminants (Fritz et al. 2000). Once separated, anions in the mobile phase are passed through an anion self-regenerating suppressor to reduce the conductivity of hydroxide ions. Suppression is necessary to remove conductive ions such as OH^- from the mobile phase in order to increase sensitivity and decrease background noise. Suppression is also necessary to remove

counter ions and to convert the ion of interest into a more conductive form, further increasing sensitivity. The suppression process begins with distilled water regenerant undergoing electrolysis to form OH^- ions and hydrogen gas (H_2) on the cathode surface while H^+ ions and oxygen gas (O_2) are formed on the anode surface. Cation exchange materials allow H^+ ions to move from the anode into the eluent chamber to neutralize OH^- ions in the mobile phase and produce water. These H^+ ions can also travel all the way to the cathode to form water. Sodium (Na^+) ions in the mobile phase are driven towards the cathode by an applied electric potential and combine with OH^- ions to form NaOH waste. Anion analytes can then move from the elutent channel in water towards the conductivity detector. The nature of ion chromatography places several constraints on the detection of ions once they are separated. Unlike other chromatographic methods where many analyte species are detectable by UV–visible spectroscopy, very few ions demonstrate this property. A common strategy applied toward the detection of ions, and in many cases the only method available, is conductivity. Conductivity detection has the major advantage in that all ions are conductive in solution; therefore, response is universal for all ions (Fritz et al. 2000).

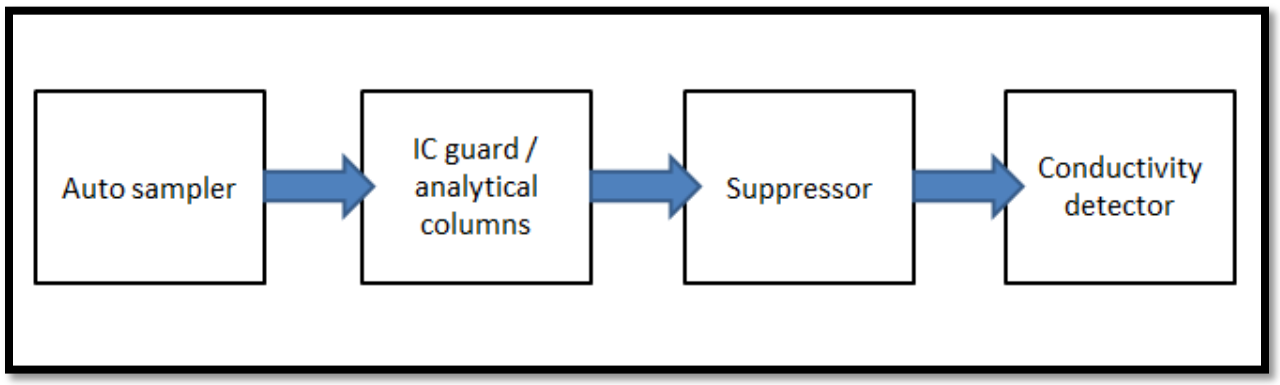

Figure 1-3. Schematic of ion chromatography – conductivity detection

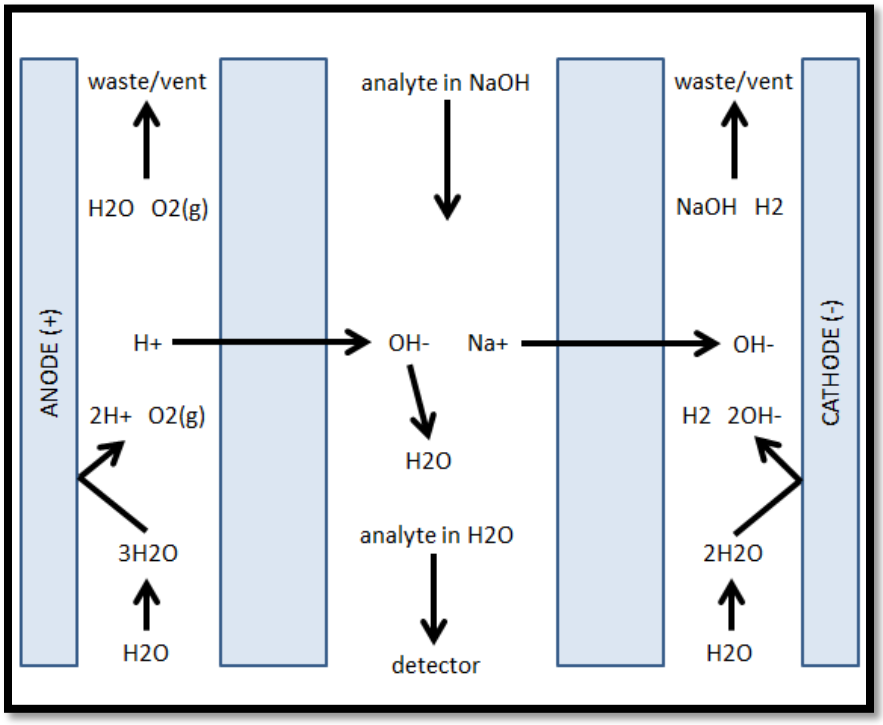

Figure 1-4. Schematic of anion regenerated suppressor

1.6.1 Negative-ion proton-transfer chemical ionization mass spectrometry

Negative-ion proton-transfer chemical-ionization mass spectrometry (NI-PT-CIMS) is described as a soft ionization technique for mass spectrometry which utilizes reactions of the acetate ion to detect organic acids such as PFCAs in ambient air. To begin, generated gas-phase PFCA samples are sampled into the NI-PT-CIMS instrument through an inlet. The gas phase acetate ion is created through a reaction between alpha particles generated with a radioactive source (polonium in this case) and acetic anhydride (Riedel et al. 2019; Veres et al. 2008). Gas phase PFCA samples are drawn from the inlet into the flow tube where they react with acetate reagent molecules. Acetic acid has the lowest gas-phase acidity of the common atmospheric acids which makes it an ideal reagent ion for the detection of organic acids via proton transfer (Veres et al. 2008):

$$\mathbf{CH_3COO^- + RCOOH \rightarrow RCOO^- + CH_3COOH}$$

The resulting analyte ions are then accelerated via ion optics towards an octopole ion guide. The octopole ion guide collimates the beam of ions and transfers them into a quadrupole mass filter which selectively filters ions based on their mass to charge ratio (m/z). By adjusting

voltages applied to the quadrupole, ions can be focused, allowing only ions of specific m/z values to pass through. An electron multiplier is then used to detect the ions (Figure 1-5). Motivations for using NI-PT-CIMS over more conventional methods such as liquid/gas chromatography include its fast, successful use in the accurate quantification of gas-phase PFCAs, smaller losses of volatile or semivolatile PFCAs during sample introduction, and selectivity towards detecting gas-phase PFCAs (Riedel et al. 2019; Veres et al. 2008). Real time in-situ measurements also allow for the quantification of fast kinetic processes such as gas-phase uptake of chemicals onto liquid/solid surfaces.

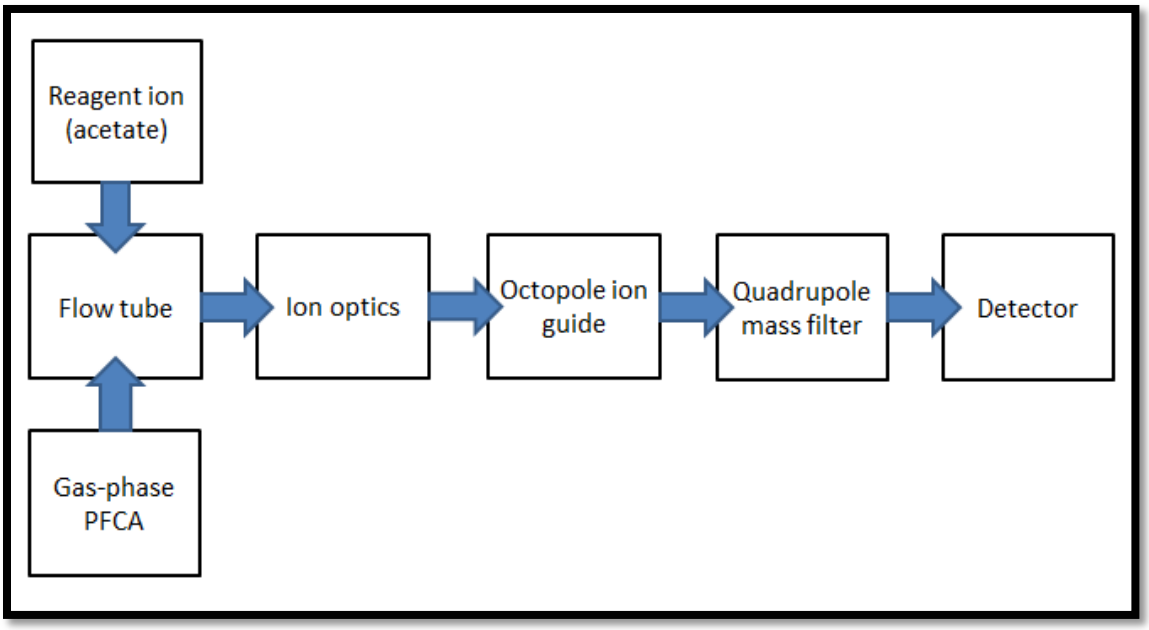

Figure 1-5. Schematic of chemical ionization mass spectrometer

1.7 Objectives of proposed research

The objective of the proposed research will be to explore the heterogeneous reactions of PFCAs with implications toward their atmospheric fate and sampling. Firstly, in Chapter 2 we will use in-situ NI-PT-CIMS to measure the uptake coefficient for an ultra-short chain PFCA, TFA. Uptake coefficients for TFA will be measured for three environmentally relevant surfaces

which include deionized water, saline water, and octanol. Deionized water will simulate uptake onto rain/cloud droplets while saline water and octanol will be used to simulate uptake onto aerosol. In Chapter 3, the capture efficiency of a short chain PFCA, PFPrA, will be characterized using annular diffusion denuders and ion chromatography. This has implications for atmospheric sampling of PFCAs.

References

Ahrens, L., Harner, T., Shoeib M., Lane, D., Murphy, J.G. 2012. Improved Characterization of Gas−Particle Partitioning for Per- and Polyfluoroalkyl Substances in the Atmosphere Using Annular Diffusion Denuder Samplers. *Environmental Science and Technology, 46, 13, 7199–7206*

Ahrens, L., Shoeib, M., Harner, T., Lane, D., Reiner, E.J., 2011. Comparison of Annular Diffusion Denuder and High Volume Air Samplers for Measuring Per- and Polyfluoroalkyl Substances in the Atmosphere. *Analytical Chemistry, 83, 24, 9622–9628*

Anwar, M., Khan, H., Lyons, K., Chhantyal, R., McGillen, M.R., Caravan, R.L., Taatjes, C.A., Orr, A.J., Percival, C.J. 2018. Investigating the tropospheric of Acetic Acid using the global 3-D chemistry transport model, STOCHEM-CRI. *Journal of Geophysical Research: Atmospheres, 123, 11, 6267-6281*

Davidovits, P., Kolb. C.E., Williams, J.T., Worsnop, J., Worsnop, D. 2006. Mass Accomodation and Chemical reactions at gas-liquid interfaces. *Chemical Reviews, 106, 1323-1354*

Duan, Y., Sun, H., Yao, Y., Meng, Y., & Li, Y. 2020. Distribution of novel and legacy per−/polyfluoroalkyl substances in serum and it's associations with two glycemic biomarkers among Chinese adult men and women with normal blood glucose levels. *Environment International, 134, 105,295*

Fritz, J.S, & Gjerde, D.T. 2000. "Ion Chromatography Third, Completely Revised and Enlarged Edition." In , 1–214. WILEY-VCH

Gewurtz, S.B., Backus, S.M., De Silva, A.O., Ahrens, L., Armellin, A., Evans, M., Fraser, S., Gledhill, M., Guerra P, Harner T, Helm PA, Hung H, Khera N, Kim MG, King M, Lee SC, Letcher RJ, Martin P, Marvin, C., McGoldrick, D.J., Myers, A.L., Pelletier, M., Pomeroy, J., Reiner, E.J., Rondeau, M., Sauve M.C., Sekela, M., Shoeib, M., Smith, D.W., Smyth, S.A., Struger, J., Spry, D., Syrgiannis, J., Waltho, J. 2013. Perfluoroalkyl acids in the Canadian environment: multi-media assessment of current status and trends. *Environment International, 59, 183-200.*

Gluge, J., Sheringer, M., Cousins, I., DeWitt, J., Goldenmen, G., Herzke, D., Lohmann, R., Ng, C., Trier, X., and Wang, Z. 2020. "An overview of the uses of per and polyfluoroalkyl substances (PFAS)." *Environmental Science: Processes & Impacts, 22, 2345*

Goss, K.U. 2008. The pKa values of PFOA and other highly fluorinated carboxylic acids. *Environmental Science and Technology, 42, 456–458.*

Guckert, M., Rupp, J., Nurenburg, G., Nodler, K., Koschorrek, J., Berger, U., Drost, W., Siebert, U., Wibbet, G., Reemstra, T. 2023. Differences in the internal PFAS patterns of herbivores, omnivores and carnivores - lessons learned from target screening and the total oxidizable precursor assay. *Science of the total environment, 875, 16231*

Johansson, J. H.; Salter, M. E.; Acosta Navarro, J. C.; Leck, C.; Nilsson, E. D.; Cousins, I. T. 2019. Global transport of perfluoroalkyl acids via sea spray aerosol. *Environmental Science: Processes Impacts. 21, 635*

Kaiser, M., Larsen, B., Kao, C-P., and Buck, R., 2005. Vapor Pressures of Perfluorooctanoic, -nonanoic, -decanoic, -undecanoic, and -dodecanoic Acids. *Journal of Chemical and Engineering Data, 50, 1841-1843*

Kutsuna, S., Hori, H. 2008. Experimental determination of Henry's law constant of perfluorooctanoic acid (PFOA) at 298K by means of an inert-gas stripping method with a helical plate. *Atmospheric Environment, 42, 8883–8892*

Kutsuna, S., Hori, H. 2008. Experimental determination of Henry's law constants of trifluoroacetic acid at 278-298K. *Atmospheric Environment, 42, 1399-1412*

Lau, C., Thibodeaux, J.R., Hanson, R.G., Narotsky, M.G., Rogers, J.M., Lindstrom, A.B., Strynar, M.J. 2006. Effects of Perfluorooctanoic Acid Exposure during Pregnancy in the Mouse, *Toxicological Sciences*, 90, 2, 510–518

Lau, C., Butenhoff, J. L., Rogers, J. M. (2004). The developmental toxicity of perfluoroalkyl acids and their derivatives. *Toxicol. Appl. Pharmacol*. 198, 231–241

Mackay, D., Ellis, D., and Li, H., 2007. Measurement of Low Air-Water Partition Coefficients of Organic Acids by Evaporation from a Water Surface. *Journal of Chemical and Engineering Data, 52, 1580-1584*

Moroi, Y., Yano, H., Shibata, O., Yonemitsu, T. 2001. Determination of Acidity Constants of Perfluoroalkanoic Acids. *Chemical Society of Japan. 74, 4, 667-672.*

Parnis, M., and Lampic, A., 2020. Property Estimation of Per- and Polyfluoroalkyl Substances: A Comparative Assessment of Estimation Methods. *Environmental Toxicology and Chemistry, 43, 775-786*

Pickard, H.; Criscitiello, A.; Spencer, C.; Sharp, M. J.; Muir, D. C. G.; De Silva, A. O.; Young, C. J. Continuous non-marine inputs of per- and polyfluoroalkyl substances to the High Arctic: A multi-decadal depositional record. *Atmospheric Chemical Physics 18, 7, 5045–5058.*

Prevedouros, K., Cousins, I.T., Buck, R.C., Korzeniowksi, S.H. 2006. "Sources, fate, and transport of Perfluorocarboxylates." *Environmental Science and Technology. 40, 1, 32-44*

Riedel, T., Lang, J., Strynar, M., Lindstrom, A., and Offenberg, J. 2019. Gas-Phase Detection of Fluorotelomer Alcohols and Other Oxygenated Per- and Polyfluoroalkyl Substances by Chemical Ionization Mass Spectrometry. *Environmental Science and Technology, 6, 289-293*

Sha, B.; Johansson, J. H.; Tunved, P.; Bohlin-Nizzetto, P.; Cousins, I. T.; Salter, M. E. 2022. Sea Spray Aerosol (SSA) as a Source of Perfluoroalkyl Acids (PFAAs) to the Atmosphere: Field Evidence from Long-Term Air Monitoring. *Environmental Science and Technology 56, 228– 238*

Shoeib, M., Harner, T., Lee, S.C., Lane, D., Zhu, J. 2008. Sorbent impregnated Polyurethane Foam Disk for Passive Air Sampling of Volatile Fluorinated Chemicals. *Analytical Chemistry, 80, 3, 675–682*

So, M. K.; Taniyasu, S.; Yamashita, N.; Giesy, J. P.; Zheng, J.; Fang, Z.; Im, S. H.; Lam, P. K. S. 2004. Perfluorinated compounds in 3536 coastal waters of Hong Kong, south China, and Korea. *Environmental Science and Technology, 38, 4056−4063*

Solomon, K.R., Velders, G.J.M., Wilson, S.R., Madronich, S., Longstreth, J., Aucamp, P.J., Bornman, J.F. 2016. "Sources, Fates, Toxicity, and Risks of Trifluoroacetic Acid and Its Salts: Relevance to Substances Regulated under the Montreal 21 and Kyoto Protocols." *Journal of Toxicology and Environmental Health - Part B: Critical Reviews, 19, 7, 289–304*

Song, M., Liu, P., Martin, S.T., Bertram, A.K. 2017. Liquid– liquid phase separation in particles containing secondary organic material free of inorganic salts, Atmos. Chem. Phys. 17, 11261–11271

Stock, N.L., Furdui, V.I., Muir, D.C.G., Madbury, S.A. 2007. Perfluoroalkyl Contaminants in the Canadian Arctic: Evidence of Atmospheric Transport and Local Contamination. *Environmental Science and Technology, 41, 10, 3529–3536*

Tang, M.J., Cox. R.A. Kalberer, M. 2014. Compilation and evaluation of gas phase diffusion coefficients of reactive trace gases in the atmosphere: volume 1. Inorganic compounds. *Atmospheric Chemical Physics, 14, 9233–9247*

Tao, Y., VandenBoer T.C., Ye, R., Young, C.J. 2022. Exploring controls on 2 perfluorocarboxylic acid (PFCA) gas-particle partitioning using a model 3 with observational constraints. *Environmental Science: Processes & Impacts, 25, 264-276*

Thackray, C.P., Selin, N.E., Young, C.J. 2020 "A global atmospheric chemistry model for the fate and transport of PFCAs and their precursors" *Environmental Science : Processes Impacts 22, 285*

US Environmental Protection Agency. 2019. CompTox Chemicals Dashboard. Washington, DC. [cited 2023 August 15th]. Available from: https:// comptox.epa.gov/dashboard/

Veres, P., Roberts, J., Warneke, C., Welsh-Bon, D., Zahniser, M., Herndon, S., Fall, R., and de Gouw, J. 2008. Development of negative-ion proton-transfer chemical-ionization mass spectrometry (NI-PT-CIMS) for the measurement of gas-phase organic acids in the atmosphere. *International Journal of Mass Spectrometry, 274, 48-55*

Wang, Z., Buser, A.M., Cousins, I.T., Demattio, S., Drost, W., Johansson, O., Ohno, K., Patlewicz, G., Richard, A.M., Walker, G.W., White, G.S., Leinala, E. 2021. "A New OECD

Definition for Per- and Polyfluoroalkyl Substances." *Environmental Science and Technology, 55, 23, 15575–15578*

Wang, Z., Cousins, I.T., Scheringer, M., Hungerbuler, K. 2013. "Fluorinated alternatives to long-chain perfluoroalkyl carboxylic acids (PFCAs), perfluoroalkane sulfonic acids (PFSAs) and their potential precursors." *Environment International, 60, 242*

Wang, Z., MacLeod, M., Cousins, I. T., Scheringer, M., Hungerbühler, K. 2011. Using COSMOtherm to predict physicochemical properties of poly- and perfluorinated alkyl substances (PFASs). *Environmental Chemistry 8, (4)*

Wu, J., Jin, H., Li., L., Zhai, Z., Martin, J.W., Hu, J., Peng, L., Wu, P. 2019. Atmospheric perfluoroalkyl acid occurrence and isomer profiles in Beijin, China. *Environmental Pollution, 245, 113129*

Xiang, Q., Shan, G., Wu, W., Jin, H.; Zhu, L. 2018. Measuring log Kow coefficients of neutral species of perfluoroalkyl carboxylic acids using reversed-phase high-performance liquid chromatography. *Environmental Pollution, 242, (Pt B), 1283-1290.*

Yamashita, N.; Kannan, K.; Taniyasu, S.; Horii, Y.; Petrick, G.; Gamo, T. 2005. A global survey of perfluorinated acids in oceans. *Mar. Pollut. Bull. 51, 658−668*

Ye, R., Di Lorenzo, R.A., Clouthier, J.T., Young, C.J., VandenBoer, T.C. 2023. A rapid derivatization for quantification of perfluorinated carboxylic acids from aqueous matrices by gas chromatography – mass spectrometry. *Analytical Chemistry. 95, 7648-7655*

You, Y. L., Renbaum-Wolff, M., Carreras-Sospedra, Hanna, S.J., N. Hiranuma, S. Kamal, M. L. Smith, X. Zhang, R. J. Weber, J. E. Shilling, D. Dabdub, S. T. Martin and A. K. Bertram. 2012. Images reveal that atmospheric particles can undergo liquid–liquid phase separations, Proc. Natl. Acad. Sci. U. S. A., 2012, 109, 13188–13193

Young, C. J. and Mabury, S. A. 2010. Atmospheric Perfluorinated Acid Precursors: Chemistry, Occurrence, and Impacts. *Reviews of Environmental Contamination and Toxicology, 208, 1-109*

Young, C.J., Furdui, V.I., Franklin, J., Koener, R.M., Muir, D.C.G., Madbury, S.A. 2007. "Perfluorinated Acids in Arctic Snow: New evidence for atmospheric formation" *Environmental Science and Technology, 41, 3455-3461*

Yu, P., Lian, S., Toon, O.B., Hopfner, M., Borrmann, S. 2022. Abundant nitrate and nitric acid aerosol in the upper and lower troposphere. Geophysical Research Letters. 49, 18.

Chapter Two:

Calculation of gas-phase uptake coefficients for TFA on various liquid surfaces using chemical ionization – mass spectrometry

D. Indos[1], C.J. Young[1]

[1]Department of Chemistry, York University, Toronto, ON, Canada

2.1 Introduction

Perfluorocarboxylic acids are a subclass of PFAS in which carbon-hydrogen bonds are completely replaced with fluorine-carbon bonds, accompanied by a carboxylic head functional group. These compounds are used in several consumer and industrial products which include non-stick cookware, food packaging, fabrics and carpets, and firefighting foams. These compounds are used for their unique chemical properties which include chemical inertness, hydrophobicity, and thermal stability (Buck et al. 2011). Upon their release into the environment these compounds (especially long chain PFCAs) are subject to slow environmental degradation and can last for hundreds of years in certain matrices such as water. These chemicals have also been shown to bioaccumulate and cause toxic effects in animals (Gluge et al. 2020). While direct emissions of gaseous PFCAs can account for their detection near point sources, they cannot for account for the detection of PFCAs in remote regions. This is because these chemicals are expected to behave like strong atmospheric acids (e.g., HNO_3, HCl) and rapidly transition into the condensed phase (rain drops or aerosol). Once in the condensed phase these chemicals can be deposited onto the surface of the earth via wet deposition (rain drops) or dry deposition (gases/aerosol) (Thackray et al. 2020).

Movement/transfer of a chemical from the gas phase into the condensed phase can be described in terms of heterogeneous kinetic and equilibrium processes. Many important atmospheric reactions involve heterogeneous interactions of gas-phase species with water droplets and aerosols. These processes begin with a gas-phase molecule colliding with a liquid surface and then entering the condensed phase (Davidovits et al. 2006; Tang et al. 2014). A parameter that can be used to describe the transfer of gases into liquids is the mass accommodation coefficient. In circumstances such as those in a lab, other processes may either limit or enhance gas-phase uptake onto a liquid. These processes include diffusion of the trace species through the gas phase to the surface, adsorption and desorption at the surface, solvation of the species and incorporation into the bulk phase, and reaction at the surface and in the bulk phase (Davidovits et al. 2006; Tang et al. 2014). Two of these processes have been found to specifically limit uptake of gas-phase molecules onto liquid surfaces and includes gas-phase diffusion limitations and solubility limitations. At equilibrium, the rate of desorption from the surface is equal to the rate of mass accommodation at the surface, yielding a net uptake of zero

(Davidovits et al. 2006; Tang et al. 2014). Once at equilibrium the movement of a chemical between two environmental compartments (e.g., air and water) can be described in terms of equilibrium partitioning. The partitioning tendencies for chemicals at equilibrium are largely determined by three equilibrium partition coefficients between air-water (K_{AW}), octanol-water (K_{OW}), and octanol-air (K_{OA}). These partition coefficients can be defined as a dimensionless ratio of a chemical's equilibrium concentration in two different compartments (e.g., $K_{AW} = C_{air} / C_{water}$) (Parnis and Lampic, 2020).

Techniques to measure PFCAs in the condensed phase have long been established; however the same cannot be said for fast (~1 sec) measurements of these compounds in the gas phase. This in turn has placed a focus on equilibrium processes/properties and how they can be used to describe the movement and fate of PFCAs in the environment. Past studies have experimentally determined several equilibrium properties for various PFCAs (though measurements are sparse) and include K_{AW} and K_{OW} (Mackay et al. 2007; Kutstuna et al. 2008; Xiang et al. 2018). Less attention however has been paid to these fast heterogeneous processes involving gas-phase PFCAs. The study of these processes is not only important in helping understand the movement of gas-phase PFCAs in the atmosphere and their possible sinks, but also in understanding the speed at which gas-phase PFCAs enter the condensed phase. Direct, fast measurements in the gas-phase can also help overcome limitations such analytical bias caused by partition losses from water samples into container walls and other laboratory materials (Lath et al. 2019). In terms of heterogeneous processes, there exists only one previous study which investigates the uptake of a gas-phase PFCA (TFA) onto water surfaces (Hu et al. 1993). From limited atmospheric measurements, TFA has also been found to be the most abundant PFCA in the atmosphere (Ye et al. 2023). Therefore, the objective of this work will be to measure uptake coefficients for an ultra-short chain PFCA, TFA, on environmentally relevant liquid surfaces using in situ negative-ion proton-transfer chemical ionization mass spectrometry (NI-PT-CIMS) measurements. These liquid surfaces include deionized water, saline water, and octanol. Deionized water will simulate uptake onto water/cloud droplets, saline water will be used to simulate uptake onto ocean surfaces and sea spray aerosol, and octanol will be used to simulate uptake onto organic portions of atmospheric aerosols.

2.2 Materials and Methods

Gas-phase standards of TFA were generated via a permeation oven with nitrogen used as the carrier gas. The permeation oven was 8" x 8" x 3" aluminum block, machined with four ½" holes designed to fit PFA flow cells, and rested on and L-shaped sheet of aluminum. This sheet of aluminum was also fitted with a process controller, solid state relay mounted on an aluminum heat sink, and 10-amp fuse. The permeation oven was mounted along the longest axis to contain a cartridge heater with an integrated K-type thermocouple housed in a high temperature sheath (300 W, 120 V, 8" length and 3/8" diameter). The set point temperature of the permeation oven was 40 ºC. Contained inside of the permeation oven was a single diluted (50:50 mix with water) TFA permeation tube which was custom-made using a 7 cm length of ¼ inch PFA tubing plugged with 0.5 cm of ¼ inch PTFE porous rods at both ends. This permeation tube was placed within 8 cm in length of ½ inch PFA tubing joined by ½ inch – ¼ inch PFA unions to connect to the carrier gas flow and glass injector. This glass injector was inserted into a custom Pyrex flow tube containing a 16 cm x 2 cm Pyrex "boat" filled with 10 mL of deionized water, saline water, or octanol (only one at a time). Deionized water was obtained in lab with the use of a reverse osmosis water filtration system (milliQ). Saline (ocean) water was created dissolving 35 grams of Instant Ocean, described as synthetic ocean salt, in 1 litre of deionized (milliQ) water. The resulting concentration of major ions were 19 g/L, 10.5 g/L, 2.7g/L, 1.3g/L 400 mg/L, and 380 mg/L for chloride, sodium, sulfate, magnesium, calcium, and potassium respectively. Also inserted into the top of the flow tube were two ¼ inch PFA tubing lines used for the dilution flow (zero air) and as a vent (denuder attached) (Figure 2-1). Flow rates for MFC 5 (dilution flow), MFC 7 (acetic anhydride flow), MFC 8 (reagent flow), and the critical orifice were set to 2500 mL/min, 50 mL/min, 2000 mL/min, and 75 mL/min respectively.

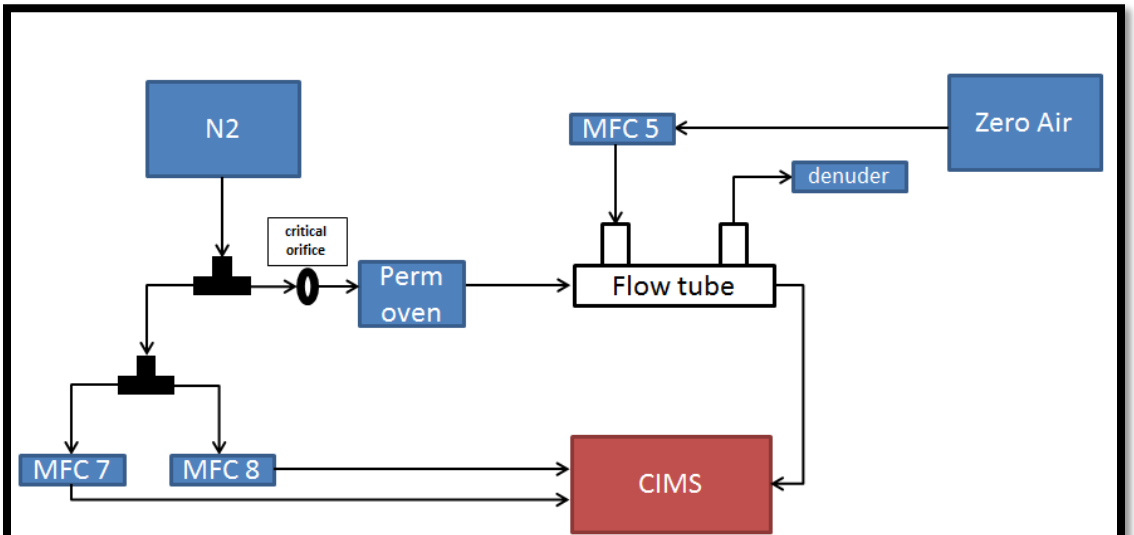

Figure 2-1. Schematic of flow tube setup for reactive uptake experiments involving TFA

Uptake experiments were carried out at room temperature (approximately 298 K) and at 0% relative humidity; however relative humidity for uptake of TFA on the surface of deionized and saline water was estimated to be close to 100% due to evaporation of water from the glass boat during uptake experiments. To begin uptake experiments the permeation oven was set to 40 ºC and the glass injector was inserted all the way into flow tube. Once the signal of TFA was stable (i.e., source output no longer increasing) a timer was started. After around 75 mins the injector was pulled back to expose the flow of TFA from the permeation oven to the Pyrex boat filled with water or octanol. The glass injector was left in this exposed position again for 75 mins (Figure 2-2). This process was repeated 5 times over the course of several days to test to evaluate the precision of our results. After each round of uptake experiments glass boats were emptied of used water and octanol and rinsed with deionized water several times. Boats were then filled with fresh deionized/ocean water or octanol for each new round of experiments. For the TFA experiments, the monitored ions included acetate (m/z 59) and TFA (m/z 113). Other monitored ions included chloride (m/z 35), nitrate (m/z 62), TFA water cluster (m/z 131), and TFA dimer (m/z 227). The signal for TFA was normalized to that of the signal of acetate. Normalization accounts for biases in TFA data due to changes in reaction processes within the flow tube.

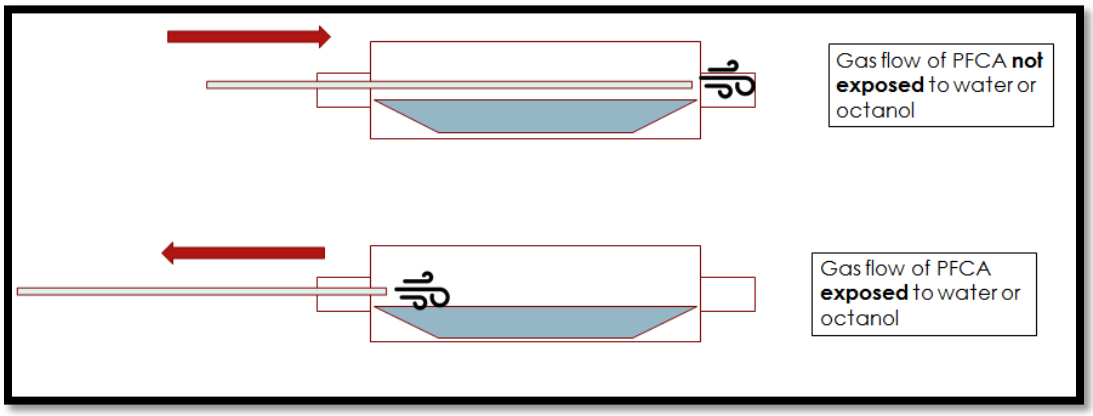

Figure 2-2. Diagram of glass injector being inserted and pulled out from the flow tube

2.2.1 Calculating uptake coefficients:

Reactive uptake efficiency of gaseous TFA to the water and octanol surface is a function of the number of collisions between the reactant and the surface, which can be determined by the residence time of the reactant (TFA) over the water and octanol surfaces. The residence time (t, seconds) spent in contact with the water and octanol surface was calculated by:

$$t = \frac{A_r \bullet d}{V_f} \qquad \text{(E1)}$$

Where A_r is the total surface area of the water and octanol (cm^2) available for gaseous TFA exchange, d is the injector distance (cm) from its initial location in the flow tube, and V_f is the volumetric flow rate (cm^3/s) of gases through the flow tube. The uptake rate was then determined using:

$$\ln \frac{C_0}{C_t} = k_m \bullet t \qquad \text{(E2)}$$

Where C_0 is the observed normalized signal of TFA with the injector fully inserted, C_t is the normalized signal with the injector at a distance, d (cm), and k_m is the measured first order loss rate coefficient (s^{-1}). Before calculating k_m, blank corrections were performed for values of C_0/C_t obtained during uptake analyses involving fresh water, ocean water, and octanol. This was achieved by subtracting the change in C_0/C_t ($\Delta C_0/C_t$) observed due to moving the glass injector from its initial position into the exposed position during blank analyses:

$$\left(\frac{C_0}{C_t}\right)_{liquid} - \left(\Delta \frac{C_0}{C_t}\right)_{blank} \qquad \text{(E3)}$$

Blanks were run the same way as uptake analyses involving water and octanol except for the fact that the glass boat was left empty instead of being filled with a liquid. As values of C_0/C_t were calculated using the signal of TFA relative to its initial, stable signal, it was not necessary

to determine the permeation rates of TFA from the custom made permeation tubes. Since these experiments were carried out at atmospheric pressure, the calculated uptake coefficient required correction for potential diffusion limitations:

$$\frac{1}{k_c} = \frac{1}{k_m} - \frac{1}{k_d} \qquad \text{(E4)}$$

Where k_d is the first order diffusion limited rate coefficient of gaseous TFA to the surface of the water and octanol and k_c is the corrected first order loss rate coefficient (s^{-1}). The value of k_d was calculated using:

$$k_d = \frac{3.6 \bullet D_{TFA}}{r^2} \qquad \text{(E5)}$$

Where D_{TFA} is the diffusion coefficient for TFA and r is the flow tube radius (0.9 ± 0.1 cm). Due to a lack of experimental data in the literature for D_{TFA}, a range of diffusion coefficients for structural analogues of TFA were used: gaseous acetic acid (0.124±0.007 cm^2/s) (Tang et al. 2015) and an average for a set of halocarbons with a similar number of carbon and fluorine atoms as TFA (0.081 cm^2/s) (Sturrock et al. 2002). The corrected rate coefficient was then used to determine the effective uptake coefficient (γ) of gaseous TFA on to a given liquid surface (deionized water, saline water, or octanol):

$$\gamma = \frac{2 \bullet r \bullet k_c}{\omega} \qquad \text{(E6)}$$

The mean molecular speed (ω, cm/s) of gaseous TFA (M = 0.114 kg/mol), using the gas constant (R = 8.314 J/mol K), and ambient temperature (T, K) was determined by (VandenBoer et al 2014):

$$\omega = \sqrt{\frac{8 \bullet R \bullet T}{\pi \bullet M}} \qquad \text{(E7)}$$

2.3 Results and Discussion

In this study the gas-phase uptake of a short-chain PFCA, TFA, onto various liquid surfaces at room temperature was investigated. For TFA uptake determination, three liquids were used as surfaces for which uptake could occur within the glass flow tube. These liquids included deionized water, ocean water, and octanol. Deionized water represents uptake onto rain and cloud droplets, saline (ocean) water represents uptake onto the surface of oceans and sea spray aerosol, and octanol can represent uptake onto organic portions of atmospheric aerosols. Rapid uptake of TFA was observed on the surfaces of all three liquids as seen in Figure 2-3. This figure demonstrates that the acetate normalized signals of TFA (normalized to the initial, stable signal of TFA) does not increase over the course of the 75 minute surface exposure and remains stable. Only when the injector is returned to its initial position does the signal of TFA return to its initial, stable value (i.e., C_t/C_0 approximately equal to 1). This indicates that TFA uptake was irreversible—the TFA did not evaporate or desorb back off the liquid surfaces. Rapid uptake of TFA was also observed on the surface of the glass boat and flow tube during blank analyses (Figure 2-3). This figure demonstrates that the uptake of TFA on the surfaces of the glass boat and flow tube is only partially reversible (that is, most is lost to the glass surface). A peak/pulse visible only when the glass injector is moved from its initial position to the exposed position during blank analyses indicates that a small portion of TFA adsorbed to glass surfaces desorbs back off. However, the signal of TFA (normalized to the initial, stable signal of TFA) does not increase further over the course of the 75 minute surface exposure, similar to uptake experiments involving water and octanol. If the uptake of TFA onto liquid and glass surfaces was fully reversible we would expect to see a small pulse when the glass injector is moved from its initial position to the exposed position (as with our blank analyses). We would also expect to see the signal of TFA slowly return to its initial, stable value even without returning the glass injector to its initial position within the flow tube. To correct for losses of TFA to the surface of the glass flow tube and boat blank corrections were performed.

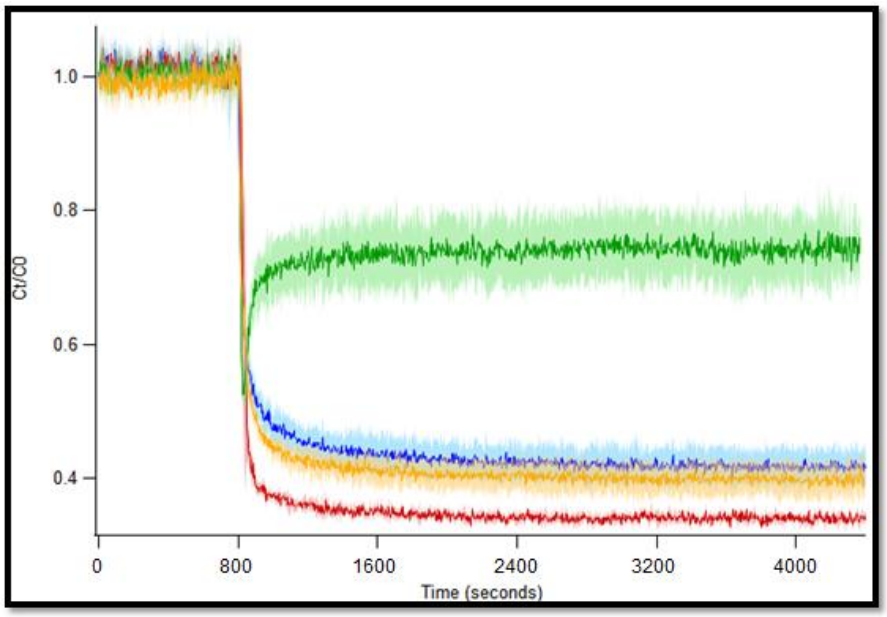

Figure 2-3. Reactive uptake of TFA onto various surfaces (injector pulled out). The green line represents the blank, blue represents deionized water, orange/yellow represents saline water, and red represents octanol. C_t/C_0 represents the acetate normalized signal of TFA normalized to the beginning of the run. Shading represents the standard (n=5)

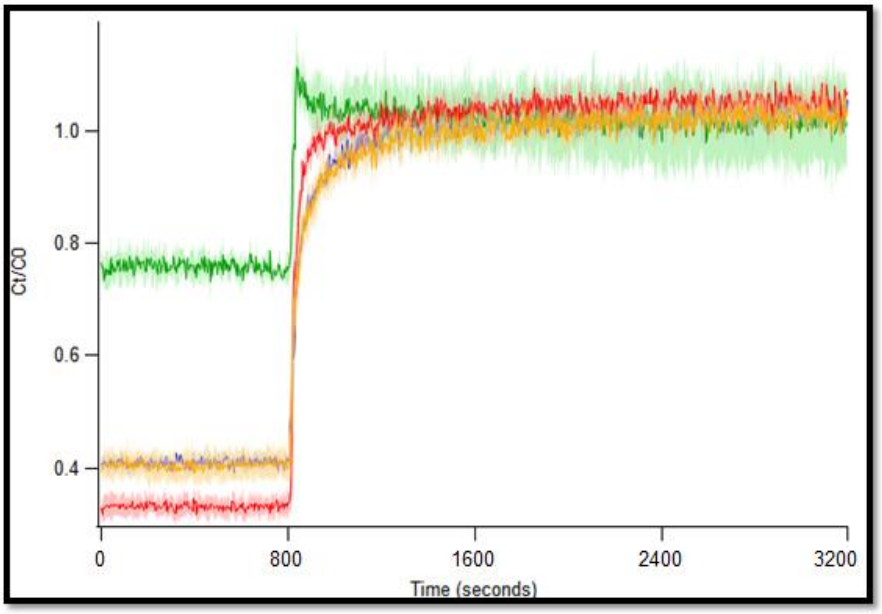

Figure 2-4. Reactive uptake of TFA onto various surfaces (injector pushed in). The green line represents the blank, blue represents deionized water, orange/yellow represents saline water, and red represents octanol. C_t/C_0 represents the acetate normalized signal of TFA normalized to the beginning of the run. Shading represents the standard deviation (n=5)

The range of uptake coefficients (calculated using diffusion coefficients for acetic acid and an average for a set of halocarbons) for TFA in deionized water, saline water, and octanol were calculated to be $2.30x10^{-4} \pm 8.57x10^{-6} - 2.37x10^{-4} \pm 8.64x10^{-6}$, $2.54x10^{-4} \pm 8.78x10^{-6} - 2.63x10^{-4} \pm 8.83x10^{-6}$, and $3.18x10^{-4} \pm 2.95x10^{-6} - 3.32x10^{-4} \pm 3.03x10^{-6}$ respectively. Reproducibility of replicates was determined by calculating percent relative standard deviations (%RSD) for each liquid surface. Calculated %RSD for fresh water, ocean water, and octanol were calculated to be 3.72%, 3.64%, and 0.92%, indicating that replicate runs for each liquid surface were highly reproducible. When comparing uptake coefficients between deionized water and saline water it was observed that saline water had slightly increased TFA uptake compared to deionized water. This slightly increased uptake of TFA into saline (ocean) water could be due to the increased pH along with the increased ionic strength of the solution compared to deionized water. However, with such a small difference between the calculated ranges of uptake coefficients for these two liquid surfaces, a t-test was needed to determine if the values were statistically different or not. The results of the t-test (p-value > 0.05) suggested that the calculated range of uptake coefficients for deionized and saline water were not statistically different. To see if pH would make any difference, calculations were also performed to determine the degree of TFA deprotonation in deionized water (pH ~5.5) and saline/ocean water (pH ~8.1). Using a pKa of 0.47 at both pHs the degree of deprotonation was calculated to be >99.99%, consistent with our observation that pH does not have a significant effect on the uptake of TFA onto water surfaces at environmentally relevant pHs (5-8). However, the ionic strength of saline/ocean water is estimated to be around 0.7 while deionized water sits close to 0. The effect of salt on the solubility of gases in seawater has been studied theoretically for a variety of small gas molecules (e.g., He, Ne, Ar, O_2, and N_2). According to particle theory, the presence of salt in aqueous solution has two important effects on gas solubility (Khan et al. 1995). These effects include a “salting-out" effect because of change in water structure and shifting the equilibrium of solute-water interactions such as dissociation, which tends to increase gas solubility. The salting-out effect is more important for larger, hydrophobic molecules, while the effect of chemical equilibrium shifting is more important for reactive species (Khan et al. 1995). A previous study investigated the effect of salinity on the air-water partitioning for several common gas-phase organic acids found within the atmosphere and included C1-C6 carboxylic acids and pyruvic acid. In all cases the presence of salt led to an increase in the activity

coefficient, therefore gas-phase solubility was decreased in saline water compared to that in pure water for these species at a given gas-phase partial pressure (Khan et al. 1995). Our observations however conclude that a change in the ionic strength of a solution does not have a pronounced effect on the heterogeneous uptake of gas-phase TFA.

Gas-phase uptake of TFA was found to be largest on the surface of liquid octanol. A suggested and likely reason for this occurrence is due to the weaker intermolecular forces, specifically hydrogen bonding, present within octanol compared to that of water. Hydrogen bonding occurs when a hydrogen atom covalently bonded to an electronegative atom (such as oxygen) is attracted to another electronegative atom. In water, each molecule can form up to four hydrogen bonds with up to four other water molecules. In octanol, while hydrogen bonding also occurs between hydrogen and oxygen atoms, the overall effect is weaker than in water due to the presence of only one positively charged hydrogen molecule and an ethyl group. This means that the energy required to form a cavity at the surface of the octanol in order to solvate a molecule is decreased as compared to water, leading to increased uptake of TFA onto the surface of octanol. To determine whether the calculated uptake coefficient of TFA onto the surface of octanol was statistically different than of that onto water a t-test was employed. The results of the t-test (p-value < 0.05) suggested that the uptake of TFA onto the surface of octanol was statistically different than that of water. This observation was also made in previous studies investigating the uptake of acetic acid onto the surfaces of water and 1-octanol. The uptake/mass accommodation of acetic acid onto the surface of 1-octanol was found to be significantly larger than of that of water. It was also noted that it took the least amount of time for TFA to desorb from surfaces within the flow tube after returning the glass injector to its initial position during uptake experiments involving octanol. This occurrence was likely due to the fact that gas-phase octanol molecules evaporating from glass boat were competing for surface sites within the glass flow tube. This prevents TFA from adsorbing to these active surface sites, therefore increasing the rate of desorption off of surfaces (specifically glass) within the flow tube.

Though not at equilibrium, TFA was likely able to reach steady state within our experimental set-up. A chemical is considered to be at equilibrium if reactants and products are both present, if the forward and reverse rate of the same reaction are equal, and if concentrations do not change over time. Chemicals are considered to be at steady state when the rate of

processes that form a species are equal to processes that remove the species. In general, steady state is used to describe kinetic processes and implies a system that is not at equilibrium; however, we can qualitatively relate our kinetic parameters to equilibrium parameters. We compared predicted values of K_{WA} ($1/K_{AW}$) and K_{OA} for TFA, and uptake coefficients calculated for TFA in this study (deionized water and octanol). In all cases, predicted values of K_{OA} for TFA were found to be larger than K_{WA} indicating that equilibrium partitioning of TFA from the gas-phase into octanol will be increased compared to that of water (Tao et al. 2022). This information is consistent with observations made during our study whereby uptake coefficients for TFA were increased on the surface of octanol compared to water.

Table 2-1. Uptake coefficients for TFA on the surface of deionized water, ocean water, and octanol calculated using diffusion coefficients for acetic acid and an average for a set of halocarbons.

Reactive surface	γ ($D_{acetic\ acid}$)	γ ($D_{halocarbon}$)	Uptake
Deionized water	$2.30x10^{-4} \pm 8.57x10^{-6}$	$2.37x10^{-4} \pm 8.64x10^{-6}$	Irreversible
Saline water	$2.54x10^{-4} \pm 8.78x10^{-6}$	$2.63x10^{-4} \pm 8.83x10^{-6}$	Irreversible
Octanol	$3.18x10^{-4} \pm 2.95x10^{-6}$	$3.32x10^{-4} \pm 3.03x10^{-6}$	Irreversible
Glass flow tube/boat	N/A	N/A	Reversible, but not fully

As this is the first study to report heterogeneous gas-phase uptake of TFA onto liquid surfaces using a flow tube and CI-MS, direct comparisons to previous studies cannot be made. However, the heterogeneous gas-phase uptake of TFA and other atmospheric acids has been previously reported using a different experimental setup (Hu et al. 1993; VanDoren et al. 1990). That study investigated the uptake of TFA onto the surface of water droplets at temperatures ranging from 263 K to 288 K. The uptake of TFA was temperature dependant with uptake onto the water surface increasing with decreasing temperature. For TFA the uptake coefficient increased from 0.044 at 288 K to 0.125 at 263 K (Hu et al. 1993). Another related study

investigated the uptake of two inorganic acids (HNO_3 and HCl) onto water droplets at temperatures ranging from 278 K to 294 K. For HNO_3 the uptake coefficient increased from 0.07±0.017 at 294 K to 0.193±0.015 at 268 K while the HCl uptake coefficient increased from 0.064±0.008 at 294 K to 0.177±0.017 at 268 K (VanDoren et al 1990).

Table 2-2. Comparison of uptake for TFA, HCl, and HNO_3 on the surface of water

Chemical/temperature	Uptake coefficient (γ)
TFA (298.5K)	$2.30x10^{-4} – 2.37x10^{-4}$
TFA (288K)	0.044 (Hu et al. 1993)
HCl (294K)	0.064 (VanDoren et al. 1990)
HNO_3 (294K)	0.070 (VanDoren et al. 1990)

For these experiments, the gas uptake was measured by passing a controlled stream of water droplets through a low-pressure flow reactor with the gas species of interest contained in a flowing carrier gas of water vapor and helium. The trace species of interest was introduced by passing helium gas through a bubbler containing the species at room temperature (Hu et al. 1993; VanDoren et al. 1990). The fast-moving stream of small, dispersed droplets (120-250um in diameter) was produced in a separate chamber by a vibrating orifice jet. The density of the trace gas was monitored downstream of the flow tube with a quadrupole mass spectrometer as the surface area of the droplets passing through the flow tube was adjusted in a stepwise fashion. The change in the trace gas signal corresponded to the uptake of gas by the droplet surface. Thus, the uptake coefficient (γ) was calculated from the measured change in trace gas signal (Hu et al. 1993; VanDoren et al. 1990). Uptake coefficients for TFA calculated this way were, in general, two orders of magnitude larger than for that of TFA calculated in our experiments at room temperature. Specific reasons for these differences are generally unknown; however differences in trace gas generation, choice of carrier gas, and experimental set-up and conditions could have played roles in these observed differences in uptake coefficients. Firstly, gas-phase PFCAs were generated through volatilization via a glass bubbler containing PFCAs. Volatilizing PFCAs this way instead of generating environmentally relevant, reproducible emissions using a permeation

oven could lead to biases in uptake data due to possible adsorption of PFCAs to the glass bubbler. Secondly, helium was used as a carrier gas as opposed to zero air. The gas-phase diffusion coefficient of TFA in helium used by Hu et al was 0.213, as compared to those used in our calculations (0.124 for acetic acid and 0.081 for an averaged set of halocarbons in air). A larger gas-phase diffusion coefficient indicates increased diffusion of TFA in helium compared to air, which may have led to an increase in uptake of TFA at the surface of the water observed by Hu et al. Thirdly, conditions such as temperature and pressure were different compared to our experimental set up. Generally an increase in temperature tends to increase the kinetic energy of gas-phase molecules, therefore increasing gas-phase diffusivity. Low pressure was also used in the experimental set up described by Hu et al. Gas-phase diffusion generally increases with decreasing pressure due to fewer collisions between other gas-phase molecules before reaching a surface. These increases in gas-phase diffusion of TFA can also lead to increases in uptake at a liquid surface. Most notably, it was not mentioned whether blank corrections were performed. As observed in our study, blank corrections were necessary to account for losses of TFA onto the surface of the glass flow tube and boat containing water and octanol. Without these blank corrections, uptake coefficients for TFA onto the surface of water and octanol could have been overestimated. To assess whether these differences would have any effect on our system, uptake coefficients for TFA on the surface of water were calculated using the same temperature and diffusion coefficient for TFA (in helium) as Hu et al. There were also no blank corrections performed for this calculation. Uptake coefficients for TFA calculated this way were slightly larger than those calculated in our experiments though still in the range of 10^{-4}. This indicates that other unknown factors may be the cause of the observed differences in uptake coefficients for TFA on the surface of water calculated here and by Hu et al.

In situations where the value of the gas-phase uptake coefficient is large, the mass accommodation process (Figure 1-2) does not limit the uptake of a gas onto a liquid surface. Instead, uptake is limited by gas-phase diffusion of the molecule towards the surface of the liquid. Our experiments were carried out at atmospheric pressure; therefore the calculated uptake coefficients required correction for potential diffusion limitations. This meant that calculated uptake coefficients were not diffusion limited. However, to determine whether the experimental system was diffusion limited equivalent uptake coefficients were calculated and compared with effective uptake coefficients for TFA calculated previously. Equivalent uptake coefficients for

TFA on the surface of deionized water, saline water, and octanol were calculated to be in the range of 10^{-3}. This is an order of magnitude larger than effective uptake coefficients calculated for TFA (Table 2-1). This indicates that our experimental system was not diffusion limited, that is, uptake of TFA at the surface of water and octanol was not limited by diffusion of TFA towards the surface of the liquids.

2.3.1 Atmospheric implications

Although the uptake coefficient of TFA onto the surface of water is two orders of magnitude smaller than those of HNO_3 and HCl it is still considered to be relatively large. This would indicate that uptake onto the surface of water and cloud/rain droplets in the troposphere is an important loss mechanism for gas-phase TFA. Uptake of TFA on the surface of saline water was similar to that of fresh water indicating that the ocean's surface (as well as the surface of sea spray aerosol) may be an important sink for gas-phase TFA in the atmosphere. The larger uptake coefficient measured for octanol surfaces indicates that TFA partitioning to organic-containing aerosol particles may also be an effective loss mechanism under some atmospheric conditions. It is recognized that organic material from both natural and anthropogenic sources makes up a large fraction of much of the fine atmospheric aerosol (Jacobson et al. 2000; Tao et al. 2022). The possibility that organic molecules adsorbed on the surface of aqueous aerosol particles may influence heterogeneous chemical processes has also been recognized. Recent measurements indicate that the organic fraction typically makes up between 1/4 and 2/3 of the mass fractions of aerosol particles with aerodynamic diameters below 1um. This is important because these particles usually dominate the aerosol particle surface area and thus control atmospheric trace gas aerosol particle heterogeneous processes (Jacobson et al. 2000; Tao et al. 2022). The partitioning of TFA to organic-containing aerosol particles also has implications for its long-range transport into remote regions such as the high Arctic due to the large distance aerosols can travel before being deposited. Like other strong atmospheric acids, overall removal of gas-phase TFA via cloud/rain droplets will likely be a more important loss mechanism within the boundary layer while removal via atmospheric aerosol will likely be more important in the upper troposphere and stratosphere. This is because the water content decreases with increasing altitude and because decreasing temperatures favor the formation of atmospheric aerosols. Similar

observations have also been made with other strong atmospheric acids such as HNO_3 whereby the mass fractional contribution of nitrates to aerosols was found to be significantly higher in the upper troposphere (30-40%) compared to near the surface (6%). Model calculations also suggested that wet deposition to be the main removal mechanism of HNO_3 near the surface (Yu et al 2022). Measured concentrations of gas-phase HNO_3 near the surface have also been found to be smaller than in the upper troposphere/ lower stratosphere (Wespes et al 2007).

References

Buck, R.C., Franklin, J., Berger, U., Conder, J.M., Cousins, I.T., De Voogt, P., Jensen, A.A., Kannan, K., Mabury, S.A. and van Leeuwen, S.P., 2011. "Perfluoroalkyl and polyfluoroalkyl substances in the environment: terminology, classification, and origins." *Integrated environmental assessment and management, 7, 4, 513-541*

Davidovits, P., Kolb. C.E., Williams, J.T., Worsnop, J., Worsnop, D. 2006. Mass Accomodation and Chemical reactions at gas-liquid interfaces. *Chemical Reviews, 106, 1323-1354*

Gluge, J., Sheringer, M., Cousins, I., DeWitt, J., Goldenmen, G., Herzke, D., Lohmann, R., Ng, C., Trier, X., and Wang, Z. 2020. "An overview of the uses of per and polyfluoroalkyl substances (PFAS)." *Environmental Science: Processes & Impacts, 22, 2345*

Hu, J.H., Shorter, J.A., Davidovits, P., Worsnop, D.R., Zahniser, M.S., Kolb, C.E. 1993. Uptake of Gas-Phase Halogenated Acetic Acid Molecules by Water Surfaces. *Journal of Physical Chemistry, 97, 11037-11042*

Jayne, J.T., Duan, S.X., Davidovits, P., Worsnop, D.R., Zahniser, M.S., Kolb, C.E. 1991. Uptake of Gas-Phase Alcohol and Organic Acid Molecules by Water Surfaces. *Journal of Physical Chemistry, 95, 6329-6336*

Jacobson, M.C., Hannson, H.C., Noone, K.J., Charlson, R.J. 2000. Organic atmospheric aerosols: review and state of science. *Reviews of Geophysics, 38, 267-294*

Khan, I., Brimblecombe, P., Clegg, S.L. 1995. Solubility of pyruvic acid and the lower (C1-C6) carboxylic acids. Experimental determination of equilibrium vapor pressures above pure aqueous and salt solutions. *Journal of Atmospheric chemistry, 22, 285-302*

Kutsuna, S., Hori, H. 2008. Experimental determination of Henry's law constant of perfluorooctanoic acid (PFOA) at 298K by means of an inert-gas stripping method with a helical plate. *Atmospheric Environment, 42, 8883–8892*

Kutsuna, S., Hori, H. 2008. Experimental determination of Henry's law constants of trifluoroacetic acid at 278-298K. *Atmospheric Environment, 42, 1399-1412*

Lath, S., Knight, E.M., Navarro, D.A., Kookana, R.S., McLaughlin, M.J. 2019. "Sorption of PFOA onto different laboratory materials: Filter membranes and centrifuge tubes. *Chemosphere, 222, 671-678*

Li, Y., Demerjian, K.L., Williams, L.R., Worsnop, D.R., Zahniser, M.S., Kolb, C.E, Davidovits, P. 2006. Heterogeneous Uptake of 8−2 Fluorotelomer Alcohol on Liquid Water and 1-Octanol Droplets. *Journal of Physical Chemistry. 110, 21, 6814–6820*

Mackay, D., Ellis, D., and Li, H., 2007. Measurement of Low Air-Water Partition Coefficients of Organic Acids by Evaporation from a Water Surface. *Journal of Chemical and Engineering Data, 52, 1580-1584*

Parnis, M., and Lampic, A., 2020. Property Estimation of Per- and Polyfluoroalkyl Substances: A Comparative Assessment of Estimation Methods. *Environmental Toxicology and Chemistry, 43, 775-786*

Sturrock, G.A., Etheridge, D.M., Trudinger, C.M., Fraser, P.J., Smith, A.M. 2002. Atmospheric histories of halocarbons from analysis of Antarctic firn air: Major Montreal Protocol species. *Journal of Geophysical Resources, 107, 4765*

Tang, M.J., Cox. R.A. Kalberer, M. 2014. Compilation and evaluation of gas phase diffusion coefficients of reactive trace gases in the atmosphere: volume 1. Inorganic compounds. *Atmospheric Chemistry and Physics, 14, 9233–9247*

Tang, M.J., Shiraiwa, U., Poschl, R.A., and Kalberer, M. 2015. Compilation and evaluation of gas phase diffusion coefficients of reactive trace gases in the atmosphere: Diffusivities of organic compounds, pressure normalised mean free paths, and average Knudsen numbers for gas uptake calculations. *Atmospheric Chemistry and Physics. 15, 5585–5598*

Thackray, C.P., Selin, N.E., Young, C.J. 2020 "A global atmospheric chemistry model for the fate and transport of PFCAs and their precursors" *Environmental Science : Processes Impacts, 22, 285*

VandenBoer, T.C., Young, C.J., Talukdar, R.K., Markovic, M.Z., Brown, S.S., Roberts, J.M., Murphy, J.G. 2014. “Nocturnal loss and daytime source of nitrous acid through reactive uptake and displacement” *Nature Geoscience. 8, 55-60*

VanDoren, J.M., Watson, L.R., Davidovits, P. 1990. “Temperature Dependence of the Uptake Coefficients of HNO_3, HCI, and N2O5 by Water Droplets”. *Journal of Physical Chemistry, 94, 8, 3265–3269*

Wespes, C., Hurtmans, D., Herbin, H., Barret, B., Turquety, S., Lazaro, J., Clerbaux, C., Coheur, P.F. 2007. First global distributions of nitric acid in the tropopause and the stratosphere derived from infrared satellite measurements. *Journal of Geophysical research, 112.*

Xiang, Q., Shan, G., Wu, W., Jin, H.; Zhu, L. 2018. Measuring log Kow coefficients of neutral species of perfluoroalkyl carboxylic acids using reversed-phase high-performance liquid chromatography. *Environmental Pollution, 242, (Pt B), 1283-1290*

Yu, P., Lian, S., Toon, O.B., Hopfner, M., Borrmann, S. 2022. Abundant nitrate and nitric acid aerosol in the upper and lower troposphere. *Geophysical Research Letters. 49, 18.*

Zhang, H.Z., Li, Y.Q., Davidovits, P., Jayne, J.T., Worsnop, D.R., Zahniser, M.S., Kolb, C.E. 2003. Uptake of Gas-Phase Species by 1-Octanol. 2. Uptake of Hydrogen Halides and Acetic Acid as a Function of Relative Humidity and Temperature. *Journal of Physical Chemistry. 107, 6398-6407*

Chapter Three:

Sampling efficiency of gas-phase PFPrA using Na_2CO_3 coated annular denuders

D. Indos[1], C.J. Young[1]

[1]Department of Chemistry, York University, Toronto, ON, Canada

3.1 Introduction

Perfluoroalkyl carboxylic acids (PFCAs) are an important subclass of perfluoroalkyl substances (PFAS) which are ubiquitously found within water bodies, the atmosphere, and living organisms. Perfluoroalkyl carboxylic acids are characterized by their resistance to environmental degradation, potential for long range transport, and accumulation/negative health impacts in plants/animals (Buck et al. 2011; Gluge et al. 2020). These compounds are also considered to be strong acids (pKa < 1). Therefore, under most environmental conditions and pHs, PFCAs exist mainly in their ionic form and are not expected to be subject to long-range atmospheric transport in the gas phase. It has been found though that a small portion of PFCAs is likely to partition to the particle phase, allowing for longer range transport as compared to gas phase PFCAs (Thackray et al. 2020). There also exist precursor molecules such as fluorotelomer alcohols (FTOHs), hydrofluorocarbons (HFCs), and hydrochlorofluorocarbons (HCFCs) which are more likely to be transported far from point sources due to their longer atmospheric lifetimes. These precursor chemicals can undergo oxidation/degradation reactions to produce a significant portion of gaseous PFCAs within the atmosphere where they can then be deposited in remote locations such as the Arctic (Young et al. 2010).

To better understand the impacts precursor molecules and particulate phase PFCAs have on the formation/deposition of PFCAs in the remote and urban environment, atmospheric sampling is necessary. Previously, PFCAs with chain lengths ranging from two carbon atoms to more than fourteen carbon atoms have been measured in the atmosphere with air concentrations ranging from low pg/m^3 in remote locations and up to a few hundred pg/m^3 in urban locations (Gewurtz et al. 2013; Stock et al. 2007). Sampling of these chemicals can be accomplished using passive and active air sampling methods. Active air sampling methods are preferred however due to the knowledge that PFCAs can exist in both the particulate and gas phase. Historically, medium/high volume active samplers utilized glass fiber filters (GFFs) and quartz fiber filters (QFFs) to sample PFCAs in the gas and particulate phase. These filters were used for their ability to strongly adsorb atmospheric acids such as PFCAs in air samples. Although these filters had their advantages at the time, several disadvantages were also reported (Ahrens et al 2011; Ahrens et al 2012).

One of the major disadvantages of using GFFs and QFFs for sampling PFCAs in air included the presence of positive sampling artifacts, resulting in an overestimation of the particle phase concentration. To avoid these sampling artifacts a new type of sampler, the annular diffusion denuder, was developed to be used with high/medium volume samplers (Ahrens et al 2011; Ahrens et al 2012). Annular diffusion denuders can be described as multichannel tubes made of glass and coated with a compound which can selectively adsorb gaseous acids (XAD-4/Na_2CO_3). In denuder samplers the gas phase is collected first followed by the particle phase, preventing the gas and aqueous phase adsorption of PFCAs to GFFs and QFFs (Ahrens et al 2011; Ahrens et al 2012). These advantages have made annular diffusion denuders the preferred method for use with high/medium volume samplers for sampling atmospheric acids, and more specifically PFCAs. Although sampling efficiency for other PFCAs and halogenated acids using annular denuders has been documented in previous studies, their efficiency at specifically sampling PFPrA has not. Sampling efficiency data from these previous studies have suggested that >98% of gaseous PFCAs flowing through the annular diffusion denuder will be adsorbed to the glass surfaces within (Martin et al. 2003; Ahrens et al 2011). Therefore, the aim of this current work will be to quantitatively determine the capture efficiency of PFPrA using Na_2CO_3 coated annular denuders and ion chromatography – conductivity detection. Capture efficiency for TFA using a preliminary method involving Na_2CO_3 coated annular denuders and chemical ionization – mass spectrometry will also be qualitatively estimated. The implications for atmospheric sampling of PFCAs will be discussed.

3.2 Materials and Methods

3.2.1 Preliminary denuder efficiency experiment (TFA/CI-MS):

A preliminary experiment involving TFA and the NI-PT-CIMS was performed prior to any official experiments where sample efficiencies were quantitatively determined using the IC-CD. Gas-phase standards of TFA were generated via a permeation oven with nitrogen used as the carrier gas. Contained inside of the permeation oven was a single concentrated TFA permeation tube which was custom-made using a 7 cm length of ¼ inch PFA tubing plugged with 0.5 cm of ¼ inch PTFE porous rods at both ends. This permeation tube was placed within 8

cm in length of ½ inch PFA tubing joined by ½ inch – ¼ inch PFA unions to connect to the carrier gas flow and an adjustable three-way valve. This three-way valve was connected to an annular diffusion denuder and a second adjustable three-way valve via ¼ inch PFA tubing. The second adjustable three-way valve was then connected to a t-joint via ¼ PFA tubing along with a separate line for the dilution flow (zero air). This t-joint was then connected to the CI-MS via ¼ inch PFA tubing. To begin this preliminary experiment, ambient air was drawn into the inlet of the CI-MS for a set period of time, acting as a blank control. The adjustable three-way valves were then set so that the flow of gaseous TFA passed through line 2. After ~10 mins the adjustable three-way valves were set to allow flow through line 1. This was repeated several times to test for variance. For reference, this preliminary experiment was meant as more of a visual aid for the official sample efficiency experiments involving PFPrA and the IC-CD, showing how denuders can effectively scrub gaseous PFCAs from the air.

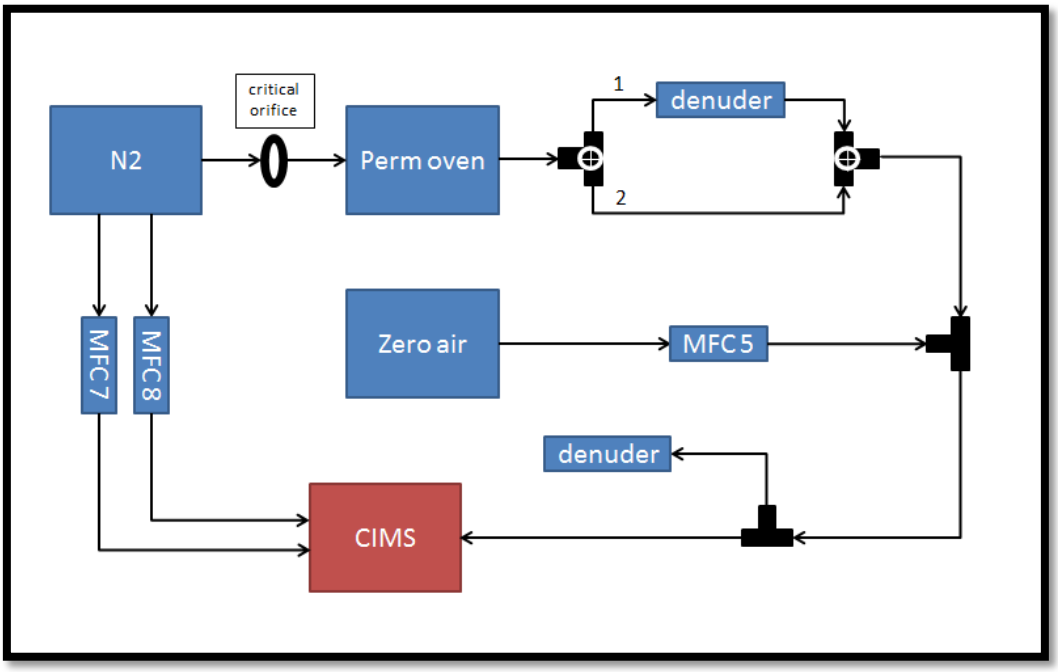

Figure 3-1. Schematic of preliminary denuder efficiency experiments using TFA/CI-MS. Lines 1 and 2 were interchangeable (only one line was running at a time)

3.2.2 Denuder sample efficiency experiments and calculations (PFPrA/IC-CD):

Gas-phase standards of perfluoropropionic acid were generated by acid displacement using potassium perfluoropropionate (K-PFPrA) and hydrochloric acid (HCl) with nitrogen as the carrier gas (MacInnis et al 2016):

$$\mathbf{HCl_{(g)} + KC_2F_5C(O)O_{(s)} \rightarrow KCl_{(s)} + C_2F_5C(O)OH_{(g)}}$$

Contained inside of the permeation oven was a 6 M HCl permeation tube and salt bed. The HCl permeation tube was custom made using 7 cm length of ¼" PFA tubing plugged with 0.5 cm of ¼" PTFE porous rods at both ends. This permeation tube was placed within 8 cm in length of ½ inch PFA tubing joined by ½" – ¼" PFA unions connected to the salt bed via ¼ inch PFA tubing. The salt bed was created by adding 0.5g of K-PFPrA to ½" PFA tubing (8cm long) filled with small pieces of 1/8" PFA tubing that were cut up to increase the surface area available for acid displacement to occur. Also connected to the salt bed were 2 separate lines made from ¼" PFA tubing which led to a bubbler filled with water. One of these lines was attached to an annular denuder (3 channels, 28mm diameter x 150mm length, 0.67lbs weight) before the bubbler while the other was not. Denuder efficiency experiments were carried out at room temperature (approximately 298K) and 0% RH. Each line was run separately for 24 hours up to three times. These samples were then sealed and stored in a fridge to be analyzed using IC-CD.

Before sample collection, denuders were cleaned by rinsing five times with deionized water, followed by a rinse with 5mL of 100% HPLC grade methanol. The denuder was then dried for 20 minutes using a flow controller attached to a nitrogen gas line. Once dried the denuder was coated with 15mL of a 2% sodium carbonate solution. This solution was prepared by mixing 500mL of optimal grade methanol, 500mL of deionized water, 20g of sodium carbonate, and 10g of glycerol. Once coated with this solution the denuder was once again dried for 20 mins using nitrogen gas (Windberry et al. 1999). Blanks simply consisted of running nitrogen through the setup into bubblers, bypassing the permeation oven.

Sealed PFPrA bubbler samples were diluted by a factor of 10 to prevent overloading the ion chromatography column. A set of standards were also created by dissolving K-PFPrA in

water and creating a series of dilutions from this mixture (0.5, 1, 5, and 10 mg/L). A Dionex AS-AP auto sampler then loaded 300µL of each bubbler sample and PFPrA standard (with loop) onto an anion concentration column (5 x 23 mm, IonPac TAC-ULP1, Thermo Scientific). Perfluoroalkyl propionic acid was separated at a flow rate of 1.0 mL/min on a Dionex IonPac AS23 analytical column (4 x 250 mm, Thermo Scientific) followed by a Dionex IonPac AG23 guard column (4 x 50mm, Thermo Fisher Scientific). The eluent used for the IC analysis was sodium hydroxide (NaOH, 50% w/w, Sigma-Aldrich). A multi-step gradient program was employed at 1mM NaOH for the first 10 minutes, increased to 2mM for 18 minutes, then further increased to 20 mM NaOH until 28 minutes, followed by re-equilibration of the analytical column by a step change to 1mM NaOH after 28 minutes, yielding a total run time of 30 minutes. The eluent was then suppressed (Dionex AERS 600, 2 mm, Thermo Fisher Scientific) before samples could be detected by conductivity detection.

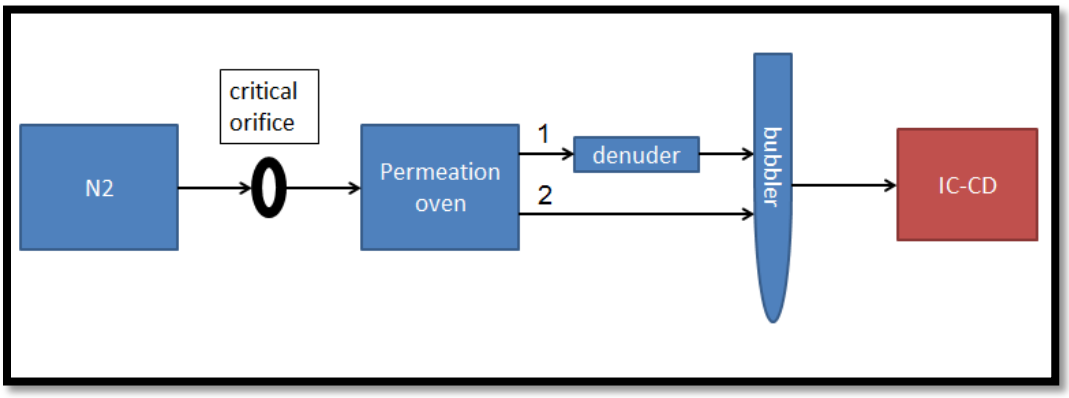

Figure 3-2. Schematic of official denuder efficiency experiments using PFPrA/IC-CD. Lines 1 and 2 were not interchangeable (only one line was running at a time).

To calculate the denuder capture efficiency the following equation was used:

$$\left(\mathbf{1} - \frac{C_{denuder}}{C_{no\ denuder}}\right) \bullet \mathbf{100}\%) \qquad \text{(E8)}$$

Where $C_{denuder}$ is the concentration of the PFPrA samples with the denuder attached and $C_{no\ denuder}$ is the concentration with no denuder attached. If $C_{denuder}$ is below detection limits, the LOD for the method detection of PFPrA using IC-CD will be used.

3.3 Results and discussion

Sampling efficiency of TFA by the Na_2CO_3 coated denuder was qualitatively estimated by passing gas-phase TFA through two sets of PFA lines attached to a CI-MS. One line was attached to a denuder (line 1) while the other was not (line 2). Gaseous TFA was produced using a permeation tube containing pure TFA acid via a permeation oven. This interaction generates stabilized, reproducible emissions of the gaseous TFA. As this was a preliminary experiment, quantitative calculations for sample efficiencies could not be performed, however qualitative estimations were made. This was accomplished by comparing the acetate normalized signal of TFA, normalized to the beginning of the run (signal count of 1) before and after switching to line 2. It was observed that the signal of TFA returned to a normalized signal of 1 after line 2 was switched back to line 1. At the very least this indicates capture efficiency of TFA using Na_2CO_3 coated denuders to be >90%. This is consistent with previous work in which capture efficiencies for TFA were quantified using Na_2CO_3 coated denuders (Martin et al. 2003).

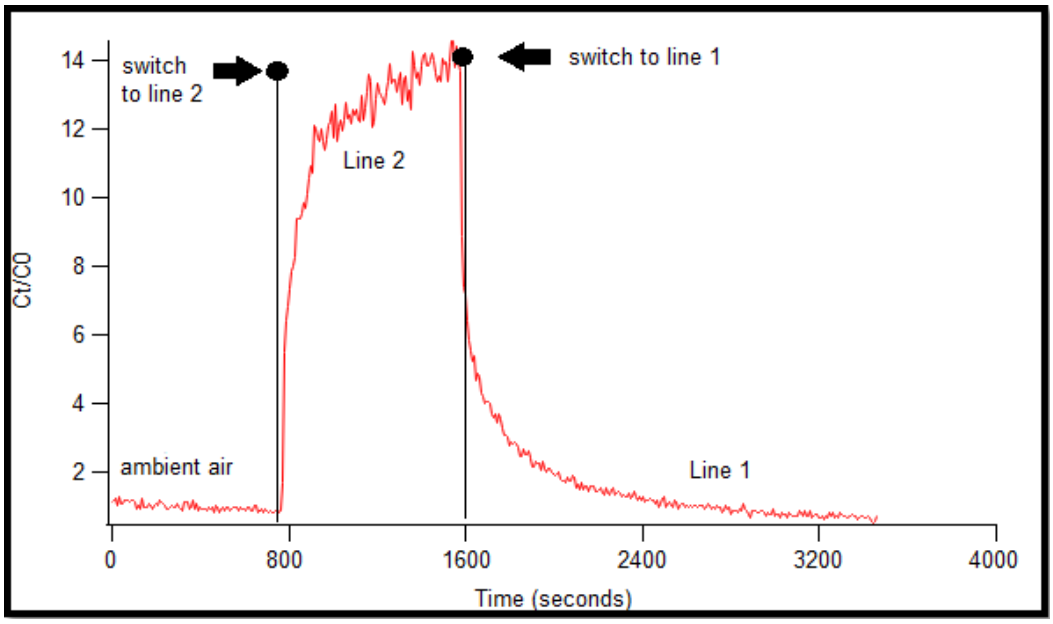

Figure 3-3. Preliminary denuder efficiency experiment involving TFA and CI-MS

Sampling efficiency of PFPrA by the Na_2CO_3 coated denuder was quantitatively determined by passing a mixture of PFPrA and zero air through two sets of PFA lines attached to bubblers. To calculate sampling efficiency the concentration of PFPrA in bubbler samples collected using line 2 (without a denuder) were compared to that of the LOD (6 ug/L) for the detection of PFPrA using IC-CD. This was due to extremely small and unquantifiable (below LOD) concentrations of PFPrA in bubbler samples run on line 1 (with a denuder). The LOD for the detection of PFPrA using IC-CD was calculated based on the following equation: (3/m) where m is the slope of a linear equation (plot of signal/noise ratio vs concentration of standards). Sampling efficiency of PFPrA by Na_2CO_3 coated annular denuders was calculated to be 99.83%±0.03%. This indicates that annular denuders are extremely efficient at sampling gaseous PFPrA from air (at a gas phase mixing ratio of 18 ppmv) during sampling.

Table 3-1. Calculated lower limits of denuder sampling efficiency for each set of PFPrA bubbler samples analyzed using IC-CD

Sample	Sampling efficiency (%)
1	99.87
2	99.81
3	99.82
Average	99.83±0.03

As this is the first study to report sampling efficiency of PFPrA using annular denuders no direct comparisons can be made. However, sampling efficiency of other PFCAs and halogenated acids using annular denuders have been previously reported. One past study reported the sampling efficiency of 6 haloacetic acids using Na_2CO_3 coated annular denuders. These 6 acids included monofluoroacetic acid (MFA), difluoroacetic acid (DFA), trifluoroacetic acid (TFA), monochloroacetic acid (MCA), dichloroacetic acid (DCA), and chlorodifluoroacetic acid (CDFA). Sampling efficiency for these 6 acids using Na_2CO_3 coated annular denuders were found to range from 82-98%. Trifluoroacetic acid (TFA) was specifically found to have a 91±5.7% sampling efficiency using annular denuders (Martin et al. 2003). To calculate the

sample efficiency for these compounds a cyclone inlet was attached to three annular denuders. Upstream of the inlet was a glass elbow used to introduce the test compounds. A sampling pump was turned on and 50uL of acetone, containing approximately 500 ng of each HAA was delivered to the glass elbow. The sample was drawn for 1 hour and each denuder was analyzed individually using GC-MS/MS (Martin et al. 2003). This procedure was repeated three times, and the mean sample efficiency on each denuder section was determined relative to the acetone spiked directly into 25mL of water. When comparing this experimental method to our own it is noted that several improvements have been made which not only increase accuracy but reduce the number of materials needed. One of these improvements includes the delivery method of PFCAs into the denuders. The use of a permeation oven offers a stable and reliable way to introduce gas-phase compounds to denuders, free of interferences caused by the presence of a solvent (Lao et al. 2020). Introducing entire quantities of PFCA over a brief period using a solvent such acetone may have resulted in less TFA adsorbing to the denuder walls, and even breakthroughs. This is because, on a molecular level, introducing a large pulse of gas-phase TFA into a denuder can over-saturate active surface sites within the denuder. Oversaturation of surface sites within the denuder can lead to gas-phase TFA passing through the denuder without being adsorbed by the coated surface, leading to a breakthrough. The use of a glass elbow to introduce TFA samples into denuders may have also led to a decrease in sampling efficiency due to the ability for glass to adsorb gas-phase acids (Furlani et al. 2022; Lath et al. 2022).

Another previous study reported the sampling efficiency of C4-C17 PFCAs onto ground XAD-4 coated annular denuders with sampling efficiencies for these PFCAs ranging from 99.64-99.99% (Ahrens at al. 2011). To calculate sample efficiencies for these compounds gas-phase PFCAs were passed through a denuder by volatilizing a known amount of PFCA from a bubbler containing water and the PFCA of interest. The amount of PFCA adsorbed to the denuder walls was compared with the amount passed through the denuder to determine sampling efficiency (Ahrens et al. 2011). When comparing this experimental method to our own involving PFPrA it was noted that they were very similar, from equations and experimental methods used, to values of sampling efficiency calculated. However, the main difference once again included the delivery method of gas-phase PFCAs to denuders. As previously mentioned, volatilizing a large amount of PFCAs all at once may lead to breakthroughs and biases in data. Permeation ovens however can provide stable, environmentally relevant emissions of gas-phase PFCAs. The use of a glass

bubbler to introduce PFCA samples into denuders can lead to biases in sampling efficiency due to PFCAs adsorbing to the bubbler. Our method therefore improves upon that of Ahrens et al by providing a more reliable gas-phase PFCA delivery method.

3.3.1. Atmospheric implications

In general, the sample efficiency calculated for PFPrA using Na_2CO_3 coated annular denuders indicates that PFPrA is efficiently scrubbed from air. This work is consistent with previous studies that have measured high sampling efficiencies for other PFCAs. The tendency for PFCAs to be scrubbed from air using Na_2CO_3 coated annular denuders can also be related to their physicochemical properties. Vapor pressures of PFCAs have been found to decrease with increasing chain length while pKa for both long and short chain PFCAs have been found to vary only slightly from one another (0.5-0.9) (Wang et al. 2011; Moroi et al. 2001; Goss et al. 2008) This indicates that it should be possible to sample long chain PFCAs with equal or greater efficiency as compared to short chain PFCAs such as PFPrA. Historically, sampling of gas-phase PFCAs in the atmosphere has been accomplished using polyurethane foam disks (often modified with added sorbent such as XAD). Data provided in our study however demonstrates that annular denuders represent a superior approach to sampling gas-phase PFCAs in the atmosphere as compared to more traditional methods.

References

Ahrens, L., Harner, T., Shoeib M., Lane, D., Murphy, J.G. 2012. Improved Characterization of Gas−Particle Partitioning for Per- and Polyfluoroalkyl Substances in the Atmosphere Using Annular Diffusion Denuder Samplers. *Environmental Science and Technology, 46, 13, 7199–7206*

Ahrens, L., Shoeib, M., Harner, T., Lane, D., Reiner, E.J., 2011. Comparison of Annular Diffusion Denuder and High Volume Air Samplers for Measuring Per- and Polyfluoroalkyl Substances in the Atmosphere. *Analytical Chemistry, 83, 24, 9622–9628*

Buck, R.C., Franklin, J., Berger, U., Conder, J.M., Cousins, I.T., De Voogt, P., Jensen, A.A., Kannan, K., Mabury, S.A. and van Leeuwen, S.P., 2011. "Perfluoroalkyl and polyfluoroalkyl substances in the environment: terminology, classification, and origins." *Integrated environmental assessment and management, 7, 4, 513-541*

Furlani, T.C., Ye, R., Stewart, J., Crilley, L.R., Edwards P.M., Kahan, T.F. 2022. "Development and validation of a new in-situ technique to measure total gaseous chlorine in air". *Atmospheric Measurement Techniques, 16, 181-193*

Gewurtz, S.B., Backus, S.M., De Silva, A.O., Ahrens, L., Armellin, A., Evans, M., Fraser, S., Gledhill, M., Guerra P, Harner T, Helm PA, Hung H, Khera N, Kim MG, King M, Lee SC, Letcher RJ, Martin P, Marvin, C., McGoldrick, D.J., Myers, A.L., Pelletier, M., Pomeroy, J., Reiner, E.J., Rondeau, M., Sauve M.C., Sekela, M., Shoeib, M., Smith, D.W., Smyth, S.A., Struger, J., Spry, D., Syrgiannis, J., Waltho, J. 2013. Perfluoroalkyl acids in the Canadian environment: multi-media assessment of current status and trends. *Environmental International, 59, 183-200*

Gluge, J., Sheringer, M., Cousins, I., DeWitt, J., Goldenmen, G., Herzke, D., Lohmann, R., Ng, C., Trier, X., and Wang, Z. 2020. "An overview of the uses of per and polyfluoroalkyl substances (PFAS)." *Environmental Science: Processes & Impacts, 22, 2345*

Goss, K.U. 2008. The pKa values of PFOA and other highly fluorinated carboxylic acids. *Environmental Science and Technology, 42, 456–458.*

Lao, M., Crilley, L.R., Furlani, T.C., Bourgeois, I., Neuman, J.A., Rollins, A.W., Veres P.R., Washenfelder, R.A., Womack, C.C., Young, C.J., VandenBoer, T.C. 2020. A portable, robust, and tunable calibration source for gas-phase nitrous acid (HONO). *Atmospheric Measurement Techniques, 13, 11, 5837 – 5890*

Macinnis, J.J., VandenBoer, T.C., Young, C.J. 2016. Development of a gas phase source for perfluoroalkyl acids to examine atmsopheric sampling methods. *Analyst, 141, 3765-3775*

Martin, J.W., Madbury, S.A., Wong, C.S., Noventa, F., Solomon, K.R., Alaee, M., Muir, D.C. 2003. Airborne Haloacetic acids. *Environmental Science and Technology. 37, 2889-2897*

Stock, N.L., Furdui, V.I., Muir, D.C.G., Madbury, S.A. 2007. Perfluoroalkyl Contaminants in the Canadian Arctic: Evidence of Atmospheric Transport and Local Contamination. *Environmental Science and Technology, 41, 10, 3529–3536*

Thackray, C.P., Selin, N.E., Young, C.J. 2020 "A global atmospheric chemistry model for the fate and transport of PFCAs and their precursors" *Environmental Science: Processes Impacts 22, 285*

Wang, Z., MacLeod, M., Cousins, I. T., Scheringer, M., Hungerbühler, K. 2011. Using COSMOtherm to predict physicochemical properties of poly- and perfluorinated alkyl substances (PFASs). *Environmental Chemistry 8, (4)*

Winberry, W. T., Ellestad, T. and Stevens, B. 1999. Compendium of Methods for the Determination of Inorganic Compounds in Compendium of Methods for the determination of Inorganic Compounds in Ambient Air, Compendium Method IO-4.2: Determination of Reactive Acidic and Basic Gases and Strong Acidity of Atmosphere

Young, C. J. and Mabury, S. A. 2010. Atmospheric Perfluorinated Acid Precursors: Chemistry, Occurrence, and Impacts. *Reviews of Environmental Contamination and Toxicology. 208, 1-109*

CHAPTER FOUR: Conclusions and future work

Chapter 2:

In this study we present a new in-situ method to quantify the gas-phase heterogeneous uptake of a short chain PFCA, TFA, onto various liquid surfaces. This method involved the utilization of a glass flow tube set-up accompanied by a CI-MS for TFA detection. Uptake coefficients for TFA were determined for three environmentally relevant surfaces which included deionized water, saline water, and octanol. As gas-phase diffusion coefficients were not available for TFA, calculations of uptake coefficients were performed using gas-phase diffusion coefficients for acetic acid and an average for a set of halocarbons. The range of uptake coefficients for TFA in deionized water, saline water, and octanol were calculated to be 2.30 – 2.37×10^{-4}, 2.54 – 2.63×10^{-4}, and 3.18 – 3.32×10^{-4} respectively. Uptake of TFA on the surface of deionized water was not found to be statistically different from that of saline water; however, the uptake of TFA on the surface octanol was found to be increased. Uptake of TFA onto the surface of fresh water, saline water, and octanol was also found to be irreversible. Comparisons between our values for the uptake of TFA on the surface of water were made to previous studies whereby the uptake of TFA, HCl, and HNO_3 were quantified for water surfaces. These comparisons showed that our calculated range of uptake coefficients for TFA on the surface of water were comparable, though two orders of magnitude smaller than those of TFA, HCl, and HNO_3 calculated in previous studies. This was likely attributed to differences in gas-phase PFCA generation, experimental set up, and methods of uptake coefficient calculation. Uptake coefficients calculated for TFA in our experiments were, however, still relatively large. This indicates uptake on the surface of rain/cloud droplets as well as liquid portions of aerosols containing salts and organic matter is an effective loss mechanism for gas-phase TFA in the atmosphere. Despite increased uptake on octanol, removal of gas-phase TFA from the atmosphere is still expected to be dominated by cloud/rain droplets.

Future work can aim to address several different topics. One of these topics includes calculation of uptake coefficients for TFA under different conditions such as varying temperature and gas-liquid contact time (carrier gas flow rate). As previously mentioned, measured uptake coefficients for TFA, HCl, and HNO_3 calculated in previous studies have been shown to be temperature dependent. Specifically, measured uptake coefficients were found to increase with

decreasing temperature (Hu et al. 1993; VanDoren et al. 1990). This trend has also been observed with other gas-phase alcohols and organic acids (Jayne et al. 1991). It is therefore important to explore the extent to which temperature influences uptake of gas-phase TFA using our experimental set-up. Gas-liquid contact times have also, to a lesser extent, been found to influence the uptake of gas-phase species onto liquid surfaces. Specifically, it has been found that increasing gas-liquid contact times leads to a very slight decrease in the measured uptake of TFA on the surface water (Hu et al. 1993). Gas-liquid contact times could be varied in our experimental set-up by either decreasing or increasing the flow rate of the carrier gas (N_2). Another topic that future work could explore includes the heterogeneous uptake of other PFCAs and atmospheric acids (such as HCl). Investigating other gas-phase PFCAs can provide information on the effects of chain length on the heterogeneous uptake of PFCAs on water and octanol surfaces. It has already been observed in previous studies that increasing PFCA chain length results in increased experimental/estimated values of K_{OW}, indicating short chain PFCAs are more likely to partition into water while long chain PFCAs are more likely to partition into octanol (organic rich media) (Xiang et al. 2018; Tao et al. 2022). Therefore, it is important to assess the effect chain length has on the uptake of PFCAs onto water and octanol surfaces, as well as to try and relate this information to equilibrium measurements (K_{OW}) made for PFCAs previously. Investigating the heterogeneous uptake other gas-phase acids such as HCl and HNO_3 are also important in helping us understand how the heterogeneous uptake of gas-phase TFA compares to other atmospheric acids. This information can help either confirm or challenge observations made in previous studies whereby uptake coefficients for HCl and HNO_3 were calculated to be extremely similar to that of TFA (Hu et al. 1993; VanDoren et al. 1990).

Chapter 3:

In this study we present a new method to quantify the capture efficiency of PFPrA using Na_2CO_3 coated annular denuders and an IC-CD. A method to qualitatively estimate capture efficiency of TFA using Na_2CO_3 coated annular denuders and a CI-MS is also briefly discussed. Capture efficiency for PFPrA was calculated by quantifying and comparing two bubbler samples run on two separate lines using an IC-CD. Line one was attached to a denuder while line two was not. As concentrations of PFPrA in bubbler samples run using line one was extremely low and

unquantifiable (below LOD), the LOD for the method detection of PFPrA using the IC-CD was used instead. Capture efficiency of TFA was qualitatively estimated by passing gas-phase TFA through two separate lines attached to a CI-MS; line one was attached to a denuder while line two was not. The acetate normalized signal of TFA, normalized to the beginning of the run (signal count of 1) was then compared before and after switching to line two. Capture of efficiency of PFPrA was calculated to be 99.83±0.03%, consistent with previous studies whereby high sampling efficiencies were observed for various other PFCAs using XAD-4 coated annular denuders (Ahrens et al. 2011). Capture efficiency of TFA was qualitatively estimated to be >90%, also consistent with a previous study whereby the sampling efficiency of TFA using Na_2CO_3 coated denuders was calculated to be ~90% (Martin et al. 2003).

Future work can aim to finalize and streamline the method for quantitative denuder capture efficiency using the CI-MS. This would allow for faster calculation of capture efficiencies for gas-phase acids as compared to the official method using the IC-CD presented in our study and methods presented in previous studies (Ahrens et al. 2011; Martin et al. 2003). This is because measurements would be performed in-situ, meaning no samples would need to be collected or analyzed using a second instrument (such as the IC-CD). Future work can also aim to quantify the capture efficiency of other gas-phase PFCAs using Na_2CO_3 coated annular denuders. Measuring the sample efficiency of larger PFCAs would allow us to understand how chain length affects the sampling efficiency of various PFCAs. This would also allow us to make comparisons to previous work whereby sample efficiencies of C4-C16 PFCAs using XAD-4 coated denuders were made and found to decrease with increasing chain length (Ahrens et al. 2011).

References

Ahrens, L., Shoeib, M., Harner, T., Lane, D., Reiner, E.J., 2011. Comparison of Annular Diffusion Denuder and High Volume Air Samplers for Measuring Per- and Polyfluoroalkyl Substances in the Atmosphere. *Analytical Chemistry, 83, 24, 9622–9628*

Hu, J.H., Shorter, J.A., Davidovits, P., Worsnop, D.R., Zahniser, M.S., Kolb, C.E. 1993. Uptake of Gas-Phase Halogenated Acetic Acid Molecules by Water Surfaces. *Journal of Physical Chemistry, 97, 11037-11042*

Martin, J.W., Madbury, S.A., Wong, C.S., Noventa, F., Solomon, K.R., Alaee, M., Muir, D.C. 2003. Airborne Haloacetic acids. *Environmental Science and Technology, 37, 2889-2897*

Moroi, Y., Yano, H., Shibata, O., Yonemitsu, T. 2001. Determination of Acidity Constants of Perfluoroalkanoic Acids. *Chemical Society of Japan. 74, 4, 667-672*.

Tao, Y., VandenBoer T.C., Ye, R., Young, C.J. 2022. Exploring controls on 2 perfluorocarboxylic acid (PFCA) gas-particle partitioning using a model 3 with observational constraints. *Environmental Science: Processes & Impacts, 25***,** *264-276*

VanDoren, J.M., Watson, L.R., Davidovits, P. 1990. "Temperature Dependence of the Uptake Coefficients of HNO_3, HCI, and N2O5 by Water Droplets". *Journal of Physical Chemistry, 94, 8, 3265–3269*

Xiang, Q., Shan, G., Wu, W., Jin, H.; Zhu, L. 2018. Measuring log Kow coefficients of neutral species of perfluoroalkyl carboxylic acids using reversed-phase high-performance liquid chromatography. *Environmental Pollution, 242, (Pt B), 1283-1290*